FAKULTÄT FÜR !NFORMATIK
Faculty of Informatics

Parallelization of BVH and BSP on the GPU

MASTERARBEIT

zur Erlangung des akademischen Grades

Master of Science

im Rahmen des Studiums

Software Engineering & Internet Computing

eingereicht von

Martin Imre, BSc.
Matrikelnummer 0853761

an der Fakultät für Informatik
der Technischen Universität Wien
Betreuung: Univ.Prof. Dipl.-Ing. Dr.techn. Werner Purgathofer

Wien, 14. Juni 2016

Martin Imre	Werner Purgathofer

FAKULTÄT
FÜR !NFORMATIK
Faculty of Informatics

Parallelization of BVH and BSP on the GPU

MASTER'S THESIS

submitted in partial fulfillment of the requirements for the degree of

Master of Science

in

Software Engineering & Internet Computing

by

Martin Imre, BSc.
Registration Number 0853761

to the Faculty of Informatics

at the TU Wien

Advisor: Univ.Prof. Dipl.-Ing. Dr.techn. Werner Purgathofer

Vienna, 14th June, 2016

Martin Imre	Werner Purgathofer

Erklärung zur Verfassung der Arbeit

Martin Imre, BSc.
Gaullachergasse 13/9-11, 1160 Wien

Hiermit erkläre ich, dass ich diese Arbeit selbständig verfasst habe, dass ich die verwendeten Quellen und Hilfsmittel vollständig angegeben habe und dass ich die Stellen der Arbeit – einschließlich Tabellen, Karten und Abbildungen –, die anderen Werken oder dem Internet im Wortlaut oder dem Sinn nach entnommen sind, auf jeden Fall unter Angabe der Quelle als Entlehnung kenntlich gemacht habe.

Wien, 14. Juni 2016

Martin Imre

Acknowledgements

First and foremost I want to thank Robert F. Tobler for offering this topic to me and being my advisor during the early stages. Unfortunately he can not see the result of my work. Next I want to thank Werner Purgathofer for taking over the role of my thesis' advisor. I want to thank the VRVis Zentrum für Virtual Reality und Visualisierung Forschungs-GmbH for providing me with the opportunity to implement my approach within one of their frameworks.

I also want to thank Stefan Maierhofer for supervising me and providing feedback throughout all phases of my work. A special thank goes to Georg Haaser and Harald Steinlechner for supporting me during the later phases. Amongst all the help received by them, I am more than thankful for countless hours of debugging and re-evaluating of ideas as well as helping with the evaluation.

Furthermore I want to thank Katharina Keuenhof for proofreading my thesis and keeping me from going insane by providing moral support, not only in form of weekly cake deliveries. Finally I want to thank all my flatmates for taking over chores and leaving food for me during the time intensive phases.

Kurzfassung

Rendering ist ein wichtiger Teil der Computergraphik und Visualisierung. Damit Bilder realistisch dargestellt werden können, sind Reflektionen, Schatten und weitere Lichtstreuungen nötig. Um diese zu berechnen, werden Techniken wie Ray-tracing, View-frustum-culling und Transparenzsortierung eingesetzt. Mit Hilfe von Beschleunigungsdatenstrukturen ist es möglich, diese Algorithmen auf die Traversierung von Baumstrukturen zu reduzieren welche auf der Graphikhardware realisiert werden können. Der Fokus dieser Diplomarbeit liegt auf zwei Datenstrukturen, nämlich Bounding Volume Hierarchies (BVH) und Binary Space Partitioning (BSP).

Üblicherweise ist es schwierig den Aufbau dieser Strukturen zu parallelisieren und die Konstruktionszeiten sind sehr hoch. Steigende Leistung und die stark parallele Architektur moderner Grafikarten (Graphic Processing Units, oder GPUs) motivieren jedoch dazu auch die Konstruktion dieser Strukturen zu parallelisieren.

In der Implementierungsphase dieser Arbeit wurden mögliche Ausgangspunkte zum Simplifizieren einer parallelisierten Konstruktion eines BSP-Baums identifiziert. Ein hybrider Algorithmus wird vorgestellt um die langen Konstruktionszeiten von BSP-Bäumen zu umgehen.

Dafür wird die Szene mit Hilfe eines uniformen Netzes in Zellen zerteilt, welche lediglich über eine kleine Anzahl an Dreiecken verfügen. Danach wird parallel in jeder nicht-leeren Zelle ein BSP-Baum gebaut. Auf diese Art kann man eine effiziente Transparenzsortierung umsetzen, in dem man zuerst die Zellen und dann die darin enthaltenen BSP-Bäume sortiert.

Die Evaluierung hat gezeigt, dass eine Erhöhung der Anzahl an Zellen im Netz nur begrenzt die Aufbauzeit reduziert. Ebenso für das Sortieren, kristallisierte sich eine Netzgröße von 25 für die beste Performanz heraus.

Der gezeigte hybride Algorithmus und die Datenstruktur versprechen die typischen Probleme einer einzelnen BSP-Baumstruktur zu überwinden. Gleichzeitig verhindern Hardwarelimitierungen aktueller GPUs derzeit noch die allgemeine Anwendung für beliebige Szenen.

Abstract

Rendering is a central point in computer graphics and visualization. In order to display realistic images reflections, shadows and further realistic light diffusions is needed. To obtain these, ray tracing, view frustum culling as well as transparency sorting among others are commonly used techniques. Given the right acceleration structure, said procedures can be reduced to tree traversals, which it is often parallelized on the graphics hardware. In this thesis we focus on Bounding Volume Hierarchy (BVH) and Binary Space Partition (BSP) which are used as such acceleration structures.

The problem with these structures is that their build time is often very high and the generation hardly parallelizable. The rising computational power and the highly parallel computation model of Graphics Processing Units (GPU) motivates to improve upon the parallelization of BVH and BSP algorithms.

Among other algorithmic exploration during the implementation phase of this thesis, possible foundation for simplifying the general problem of BSP-Tree generation in parallel has been made. A hybrid algorithm is introduced to bypass the long construction time of BSP-Trees by reducing the problem size to a small amount.

The scene is split via the usage of an uniform grid so that every cell contains only a small amount of triangles. Then a BSP-Tree is built in each of the grid's nonempty cells in parallel. Thus transparency sorting can be done by first sorting the cells and then the small BSP-Trees.

Evaluation showed that increasing the number of grid cells only leads to a decrease in build times up to a certain point. Also for sorting, the performance peaks around a grid size of 25 and decreases thereafter.

The explained hybrid algorithm and its data-structure seem to theoretically overcome typical problems of the single BSP-Tree generation. However, limitations of the GPU still have a high influence on this procedure.

Contents

Kurzfassung **ix**

Abstract **xi**

Contents **xiii**

1 Introduction **1**
1.1 Rendering . . . 1
1.2 Acceleration Structures . . . 3
1.3 Graphics Processing Unit . . . 3
1.4 Goal Of Thesis . . . 4

2 Related work **5**
2.1 Bounding Volume Hierarchy . . . 5
2.2 Binary Space Partitioning . . . 7
2.3 Tree Traversal . . . 7

3 Background **9**
3.1 Rendering . . . 9
3.2 Bounding Volume Hierarchy . . . 11
3.3 Binary Space Partitioning . . . 17
3.4 Parallel Random-Access Machine. . . . 20

4 OpenCL **25**
4.1 Introduction . . . 25
4.2 History . . . 25
4.3 Architecture . . . 26
4.4 Code Example . . . 28
4.5 Usage . . . 29

5 Implementation **33**
5.1 Bounding Volume Hierarchy . . . 33
5.2 Binary Space Partitioning . . . 38
5.3 Limitation Of The GPU . . . 52

6 Evaluation **57**
6.1 Setup 57
6.2 Root Node Selection 59
6.3 Grid Size 60
6.4 Comparing Implementations 62

7 Conclusion and Future Work **67**
7.1 Future Work 68

List of Figures **69**

List of Tables **70**

List of Algorithms **71**

Bibliography **73**

CHAPTER 1

Introduction

1.1 Rendering

Computer generated images are becoming more realistic every day. Yet they are not perfect and take some time in advance to be computed. Although hardware is still improving from one generation to the next, it still takes quick algorithms to compute these images within a short time.

Realistic images typically consist of several fine details such as reflections, shadows and other light diffusions. Since these are generally not easy to calculate for a whole image, it is split in smaller parts. These splits are then organized in so-called acceleration data structures which offer fast traversal. A typical use for traversing such a structure would be ray tracing, frustum culling as well as transparency sorting.

1.1.1 Ray Tracing

Ray tracing is a central algorithm in the domain of rendering. Arisen in the 1970s, it is still used when it comes to calculating reflections, shadows and transparencies in generated scenes. When applying ray tracing — roughly speaking — an eye ray is sent into the scene where it is reflected, absorbed, or goes through objects. In order to calculate those intersections the ray has to be checked against every object in the scene. Since the amount of objects in a scene has risen enormously since the introduction of ray tracing, it is necessary to simplify this procedure. In Figure 1.1 a figurative example for ray tracing is shown.

1.1.2 Culling

View frustum culling is used to determine which objects of a given scene have to be displayed. When it comes to rendering, a scene is often bigger than what is displayed. It

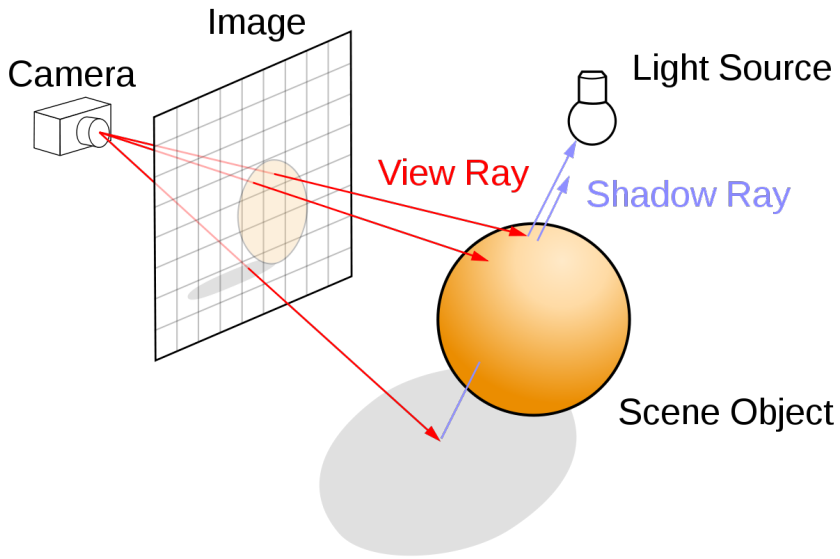

Figure 1.1: Ray tracing example [Hen08]

is therefore needed to evaluate what will be seen from a given point of view. Through culling it can easily be obtained which objects needs to be rendered and which can be completely ignored for the current view point.

1.1.3 Transparency Sorting

For realistic images it is typically needed that some objects have to be (half-)transparent. In order to render these transparencies efficiently, a back to front rendering is applied. This implies that the transparent objects need to be sorted in the order of their appearance. For this process several transparency sorting algorithms are applied, depending on the scene details. Figure 1.2 shows an example of one of these algorithms.

(a) Image with alpha blending

(b) Image with transparency sorting

Figure 1.2: An example for transparency sorting from AMD's Mecha demo [AMD], in the left image (a) alpha blending leads to the wrong result, while in in the right image (b) transparency sorting yields the correct one

1.2 Acceleration Structures

As already mentioned in the introduction (Section 1.1), acceleration structures are used to achieve the formerly described parts of rendering in a fast way. These structures are characterized by fast and cheap traversals and good approximation of real objects in a scene. In this thesis we focus on *bounding volume hierarchy* (BVH) and *binary space partitioning* (BSP) which will be introduced in section 1.2.1 and section 1.2.2 respectively. Further acceleration structures that are generally used are the k-d tree as well as the quadtree and the octree which are special cases of the BSP.

1.2.1 Bounding Volume Hierarchy

The bounding volume hierarchy is a simple binary tree structure. Generally speaking it is a hierarchy which uses the minimum bounding box of the objects in the scene. The root node contains the whole scene and is split into two parts. The children contain the bounding box surrounding all objects in either side of the split. The hierarchy goes further down recursively until the nodes only hold the bounding box of a single object. When traversed, it offers the possibility to exclude a large set of object quite fast. This helps to reduce the number of checks for a given operation (e.g. ray tracing's intersection tests). Further details about the BVH are elaborated in section 3.2.

1.2.2 Binary Space Partitioning

Another acceleration structure is the binary space partitioning tree. With the BSP algorithm the scene is separated into several disjoint regions. This is done via split planes through the scene. Each of the planes separates the scene into two regions which are further split recursively. This procedure is done until a certain end criteria is met. The traversal of the resulting in a BSP-Tree is faster than the ones of the BVH-tree. This speedup comes with the drawback of a longer buildup time. In section 3.3 we will go further into detail about the BSP.

1.3 Graphics Processing Unit

Within the last decades the computation power of graphic hardware (graphics processing unit (GPU)) has increased enormously. The GPU is designed to read and write memory in a fast fashion. It further is built with a highly parallel structure. Originally conceived for rendering with rasterisation methods, it was made accessible for general purpose computing (GPGPU [gpg]) in the early 2000s. Through further improvements on the support for accessing the vast parallel computational power of a GPU, it has become common practice to do further rendering calculations — such as ray tracing — with it. Its ample capability to parallelize tasks needs to be considered when designing algorithms in order to leverage its full power. In section 3.4 further details of the parallel computational model will be explained.

1.4 Goal Of Thesis

With this thesis we aim to improve the aforementioned algorithms and implement them for the GPU. The practical part of this thesis will be laid out within the OpenCL framework. It further will contain a higher level of accessibility to use the implementation within an F# or C# environment. As framework for the higher level handles the Aardvark rendering framework of VRVis will be used. The general goal is to construct and implement efficient and fast algorithms for BVH-and BSP-tree construction as well as traversal within the OpenCL. The reason for this is that we want to bypass the data transfer between the CPU and the GPU during rendering.

The desired use case for the BVH-tree was frustum culling and transparency sorting with the BSP-Tree. Throughout the implementation stage we came across certain road blocks and had insights showing that the starting idea would lead to unnecessary overhead. After reevaluation on the already implemented details and the plan for this thesis we came to a solution for each of the desired use cases. For frustum culling we will just evaluate every triangle in parallel. For transparency sorting we are using BSP-Trees after separating the input scene into small cells with the use of an grid. Further details about BVH-tree and BSP-grid generation will be explained Chapter 5.

CHAPTER 2

Related work

2.1 Bounding Volume Hierarchy

Since automatic generation of bounding volume hierarchies was introduced by Goldsmith et al. [GS87] in 1987 an ample amount of advances have been made in this field. In the beginning there where several heuristic approaches used for the creation of BVH-trees. Goldsmith et al. not only introduced the idea of automatically generated BVH but also suggested different heuristics. Among their proposal one could find the general idea of adding the node which leads to the least increased surface area. This — so-called — *surface area heuristic* (SAH) is now commonly used in the generation of BVH-trees. Ize et al. [AKL13] developed different measures to further analyze the quality of a BVH-tree. Unfortunately the use of these metrics is not common and sometimes not possible during construction.

2.1.1 Construction Methods

Throughout the last decades several approaches for generating a BVH-tree on the central processing unit (CPU) as well as on the GPU have been introduced. The typical algorithm in this case a top-down construction. These top-down methods [GS87, Wal07, KIS$^+$12, BHH15a] commonly start with the whole scene as root node and continue splitting it until only the nodes of the BVH-tree consist of as single object. Further bottom up methods have also been considered and used [WBKP08, GHFB13, BHH15b]. In the case of agglomerative clustering approaches the leaves are first created containing a single geometry. The next step combines two leaves together to and connects them with a parent node. Further those nodes are then connected in a recursive fashion until they result in a full BVH-tree.

2.1.2 Parallel Construction

Alongside the already mentioned methods, huge ameliorations and innovations have been made in the area of parallel construction of BVH-trees. Ize et al. [IWP07] showed an approach where the BVH-tree is created asynchronously. This way they tackle the problem of the degrading quality of a BVH throughout the lifetime of a scene.

Lauterbach et al. [LGS+09] introduced two construction algorithms. Their first method used a linear ordering from a Morton code[1], while the other one uses a top-down approach which employs the surface area heuristic. Further they combined both algorithms and removed bottlenecks for them to work on the GPU.

Pantaleoni et al. [PL10] introduced a combined approach which leverages the a greedy SAH approach as well as the LBVH approach of Lauterbach et al. [LGS+09].

Soping et al. [SBU11] altered the BVH generation algorithm and split it into single tasks. These separate tasks are then completed in parallel when the method is run on a GPU. They reported speedup up to five times in comparison to Lauterbach's algorithm.

Karras [Kar12] introduced a new method for generating a BVH-trees as well as octrees and k-d trees. Their main contribution was the creation of a radix tree which they used for their final construction algorithm. The full procedure leans on Lauterbach et al.'s method by also using the Morton codes and then sorting them with said radix tree. Further contributions are the building of a BVH-tree and further assigning bounding boxes to every internal node in parallel.

Later Karras et al. [KA13] introduced a new algorithm that leverages the capabilities of parallel computation for tree optimization. They first generate at BVH-tree and perform a set of optimizations on it. After these adaptations of the original tree are done, a post-processing step to further enhance the quality of the final BVH-tree is executed.

2.1.3 Update Based Techniques

Since the quality of a BVH has a huge influence of the traversal performance, several update methods have been proposed. These updates (e.g. refitting, tree rotations) were originally used in off-line[2] construction. Kopta et al. [KIS+12] adapted those techniques to also work on animated scenes. They improve the quality of a BVH by rearranging nodes in the tree instead of rebuilding the whole tree during the refitting phase. Further they added different variations of their algorithm and showed that they can accomplish major improvements to former algorithms.

Another interesting approach was introduced by Ernst et al. [EG07]. Clipping the triangles in the scene before creating the BVH itself allows the creation of higher quality BVH-trees. This approach is commonly used amongst the newer construction methods.

[1] The Morton code is a way to encode multidimensional data in one dimension

[2] on-line construction happens at run time, while off-line methods work in advance

2.2 Binary Space Partitioning

Since binary space partitioning was introduced in 1969 by Schumacker et al. [SD69], several advances have been made. A decade later Fuchs et al. [FKN80] used the approach in the area of computer graphics. From there on different developments where made. Chin et al. [CF89] showed how to use multiple BSP-Trees for shadow generation. Ize et al. [IWP08] leveraged the possibilities BSP-Trees offer for ray tracing. Uysal et al. [USC13] applied BSP for hidden surface removal. They have also showed how to implement it on in a parallel way with CUDA. Another interesting approach is the RBSP by Budge et al. [BCNJ08]. Their algorithm restricts the allowed split plane at each level and therefore speeds up the construction significantly.

Further restriction of the BSP leads to k-d trees. Since their construction time is more adequate for real time usage they have been studied more thoroughly within the domain of rendering. In 2007 Shevtsov et al. [SSK07] introduced algorithms to construct and traverse k-d trees in parallel. A year later Zhou et al. [ZHWG08] presented the first parallel implementation of a k-d tree on the GPU. Doggett et al. [CKL$^+$10] showed how to incorporate the SAH into the k-d tree construction in a parallel fashion. With Wu et al. [WZL11a] a year later the first implementation of a SAH generated k-d tree on the GPU was published. This year Yang et al. [YYWX16] introduced a new method — the multi-split k-d tree — that exploits ideas of the octree and allows faster high quality generation of a k-d tree in parallel.

Arya [Ary02] analyzed BSP's worst case height and size in the case of axis-parallel line segments. Further Hershberger et al. [HS03] showed additional complexity bounds.

Since BSP being a general data structure used in many fields, several advances have been made. Listing them all would be beyond the scope of this thesis; at this point we refer an interested reader to Tóth [Tót05] report.

2.3 Tree Traversal

The main focus of this thesis lies on the two acceleration structures (BVH and BSP). However it is also important to mention what has been changed throughout the last decades in the area of traversal methods and applications. Due to the parallelism in nowadays' GPU architectures a common method — using a stack — has become suboptimal when it comes to memory footprint. Foley et al. [FS05] introduced two methods to traverse a tree without a stack: *KD-Restart* and *KD-Backtrack*. To overcome the increase of visited nodes and the back pointer problem of these methods respectively, *KD-Jump* [HL09] was introduced. This technique tricks by using a small stack-like structures with only a few integers. Also a hybrid algorithm of the stack based method and the KD-Restart has been proposed. The so-called *short stack* uses a small stack to overcome memory usage and reverts to KD-Restart in certain cases.

Another interesting technique proposed already in the 90s is using *ropes* while traversing. MacDonald et al. [MB90] introduced the *rope trees* and their usages in ray tracing

traversal. Later Havran et al. [HBZ98] implemented said technique and showed that it leads to a speedup during the traversal phase. These so-called ropes link leaves of a BSP-Tree to their neighbors. Here the fact that at a given node a splitting plane prunes one dimension is abused. Therefore the rope tree created at that leaf is just two-dimensional. They showed that the construction of ropes is bounded by $O(n \log n)$ with n denoting the number of leaves in the original BSP-Tree. They further showed that the construction of rope trees lies in $O(n)$. Therefore the complexity during BSP construction is not increased, while the traversal cost is reduced drastically. Unfortunately there is no further research in parallelization of these rope trees.

A special mention here goes to Andrysco et al.'s *matrix tree* [AT11]. Based on Andrysco et al. [AT10] they built a data structure which achieves $O(1)$ insert and leaf finding. They further showed how to extend their structure in order to use it as general representation for BSP-Trees

CHAPTER 3

Background

3.1 Rendering

As already mentioned in Section 1.1 it takes an ample amount of calculations to obtain a realistic scene. In this section we will describe how rendering takes place. The first — and most naive — rendering algorithm was the *painter's algorithm*. When used, the painter's algorithm first sorts the polygons in the scene by their distance to the viewpoint. In the next step those objects are rendered back to front. Although it displays the correct image, it often re-renders certain parts of the image and is not suitable for transparencies. In case of overlapping structures it further runs into a hurdle while sorting back to front as shown in Figure 3.1.

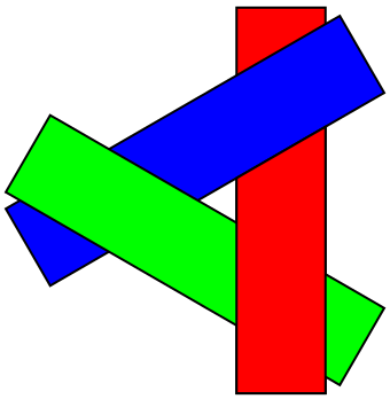

Figure 3.1: Overlapping objects or polygons can cause the painter's algorithm to fail [Muł]

The next step in terms of rendering algorithm was ray casting. Introduced by Appel [App68] in 1968 it was the first ray tracing algorithm. The main flow of the algorithm

is shooting a — so-called — eye ray from the position of the viewer in order to find the closest intersecting object. This object's properties — such as material or transparency — are then inspected and the object is drawn. This process is repeated for every coordinate along one axis. The ray casting algorithm therefore draws from left to right (using the x-axis) and therefore does not need to overdraw certain areas. Although this saves time, a major drawback is that finding intersections is needed. This may take a long time since every object in the scene has to be tested. A schematic example of how the algorithm works can be seen in Figure 3.2 whereas Figure 3.2a shows a 2-dimensional example and Figure 3.2b displays the 3-dimensional case.

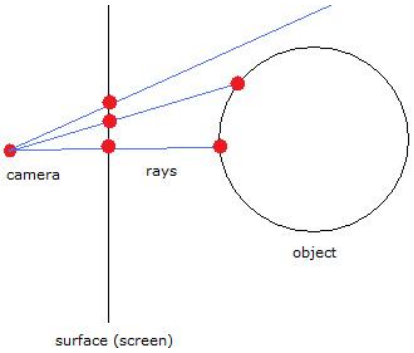

(a) Ray casting example 2D [Ado]

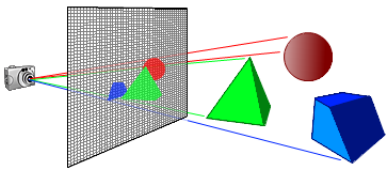

(b) Ray casting example 3D [imga]

Figure 3.2: These images show ray casting in 2D (a) and 3D (b)

The next improvement in the rendering domain was using the ray casting algorithm in a recursive manner. This procedure is called *ray tracing* algorithm. Like in ray casting, a ray is shot from a given starting point (e.g. the eye position of the viewer). Upon intersection with an object, it is evaluated whether the object emits further rays or not. In Whitted's [Whi79] algorithm it is possible that a ray generates up to three new rays when intersecting an object. These rays could be *reflection*, *refraction* and *shadow rays*. In case of reflection the ray tracing restarts at the intersection point and goes into the mirrored direction. When it comes to refraction the ray continues traveling through the material and may exit it. Shadow rays are shot into the direction of each light of the scene. In case an opaque material blocks the direct way to the light, the object lies in the shadow. Figure 3.3 shows the three possibilities that can happen upon ray intersection.

Although the ray tracing algorithm is capable of generating very realistic images (one example shown in Figure 3.4), it has a major drawback when it comes to execution time. Because it is necessary to shoot one ray for every pixel in the image and recursively emit rays upon object intersection, it is computationally infeasible to apply a naive ray tracing for complex scenes or real time image generation.

Since this problem can not be solved by omitting rays the need for a faster procedure is given. This issue is tackled by using acceleration structures such as BVH, BSP which

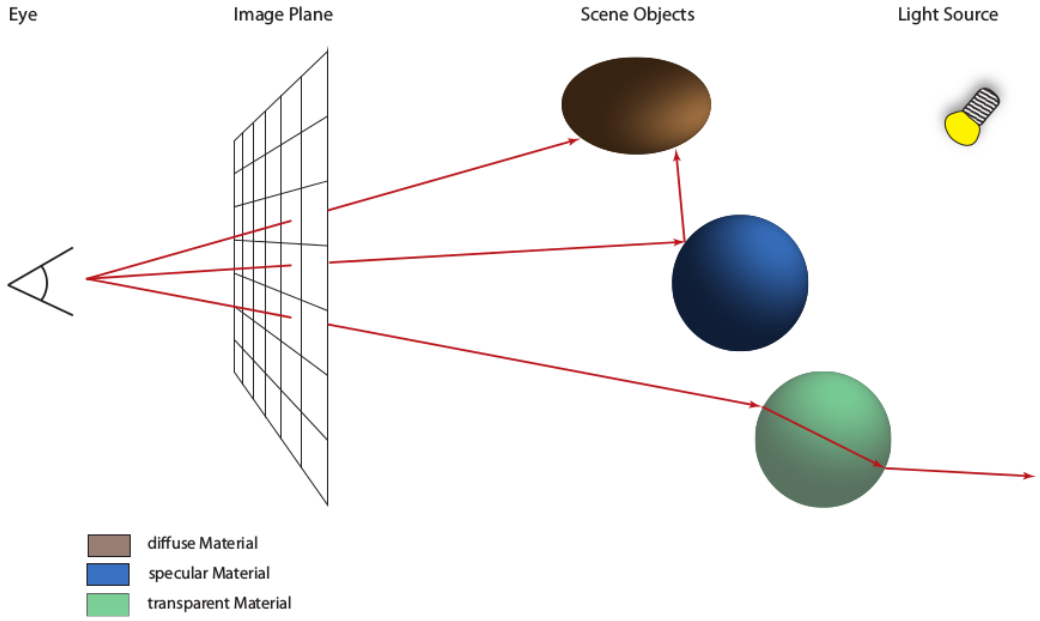

Figure 3.3: A schematic example of how the ray tracing algorithm works [Vog13]

will be explained in Section 3.2 and Section 3.3.

There exist further algorithms for rendering such as the *scanline algorithm* and *rasterization*. The former one goes through a scene line by line and renders the frontmost objects or polygons. The latter one subdivides the scene into a grid and subsequently goes through the grid and checks each cell for primitives to render. Since these algorithms lie outside the focus of this thesis we will not further discuss them here.

3.2 Bounding Volume Hierarchy

The bounding volume hierarchy is a simple acceleration structure. There are several approaches on how to build a BVH-tree where the original one was top-down. In case of the top-down generation a bounding box containing the whole scene is created to begin with. In the next step this bounding box — which is also the root node of the resulting BVH-tree — is split into half. Each of these halves represent a tighter bounding box to their containing objects. These new nodes in the tree are then further subdivided recursively. This happens in the same manner as with the root node until a certain end criteria is met (e.g. a node contains only one object).

Figure 3.5 offers a 2-dimensional example of a bounding volume hierarchy. The scene in Figure 3.5a contains five bounding boxes, whereas the bigger ones are named **A**, **B** and **C**. **B** is further split into 2 unnamed bounding volumes. Figure 3.5b displays the tree

Figure 3.4: Example image for ray tracing [Trab]

equivalent of the scene. The BVH-tree has **A** as root node. Its children are **B** and **C**. The former one split itself another time while the latter one already only contains two children which are objects. The child nodes of **B** also contain only objects which end up being leaf nodes.

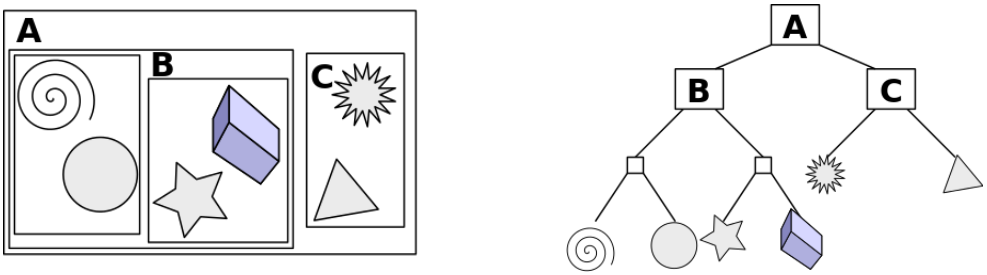

(a) Scene divided into bounding boxes

(b) Resulting BVH-tree

Figure 3.5: A 2D example [Sch] for a bounding volume hierarchy (a) and the according BVH-tree (b)

In case of bottom-up construction the algorithm takes single objects (or their bounding volume) as starting point. Then the two closest objects are put together within a new bounding box. With this step the leaves of the BVH-tree — again presented by the objects — obtain their parent nodes. This is continued recursively until there is only one bounding box left, which contains the whole scene.

In the example shown in Figure 3.5 first the single objects are taken and for each a leaf of the BVH-tree is created. Then each leaf object searches the next closest object and a bounding volume is spanned upon them. The newly generated bounding box is equivalent to a parent node in the BVH-tree. This is continued recursively to obtain **B** and then further create the root node **A**.

Both of the generation fashions have their advantages and drawbacks. On the one hand the top-down algorithm deals with the problem of finding a good splitting point at every level of recursion; while on the other hand the bottom-up method needs to find the closest object in order to combine two nodes.

Before going into detail on how exactly a BVH-tree is generated we will first discuss the requirements it has to fulfill.

It is very important that — after the construction — the obtained BVH-tree has a high quality. The quality of a BVH is vaguely defined by the time it takes to traverse it (e.g. in ray tracing, the traversal time of rays). Furthermore fast construction is required — especially in real-time rendering. In case the BVH is used in a real-time scenario shorter build times are often more valuable than perfect quality. Hence BVH-trees used in these settings suffer from a quality vs. speed trade-off. Another requirement is a small memory footprint. This is very crucial when it comes to parallel implementations since they often suffer from unbalanced or badly organized memory.

3.2.1 Construction

The examples in the last section already showed roughly how a BVH-tree is built. Nevertheless various algorithms have been proposed to speed up certain steps during the construction phase. Most algorithms commonly use the surface area heuristic which was introduced by Goldsmith et al. [GS87] and is defined as followed:

$$SAH := \frac{1}{A_{root}}(C_{inn} \sum_{n \in I} A_n + C_{tri} \sum_{n \in L} T_n A_n) = \sum_{n \in N} C_n \frac{A_n}{A_{root}} \tag{3.1}$$

In Equation (3.1) A_n describes the surface area of a certain node n, N the set of nodes split into the inner set I and the leaf nodes L. C_{inn} describes the costs for traversing an inner node (i.e. two ray-node tests), while C_{tri} are the costs for a ray-triangle test. C_n describes the cost for processing a node n and T_n is the number of triangles in said node. The fraction $\frac{A_n}{A_{root}}$ therefore is the probability of a ray intersecting a node n.

This heuristic is commonly used to speed up the construction process since the building of an optimal BVH-tree is assumed to be an *NP-hard* problem. In a recent report Aila et al. [AKL13] analyzed the correlation between the SAH and the ray tracing performance of the resulting tree with several building algorithms. They used multiple scenes for every algorithm and studied the correlation between the estimation through SAH and the quality of the BVH-tree thoroughly. Throughout their inspection they observed that the said correlation is far from perfect and that SAH often mispredicts

the outcome. Nevertheless they also noticed that top-down sweep-based algorithms often underestimate the actual performance when using the SAH. Although Aila et al. proposed two new measurements[1] for the quality of a BVH-tree, neither of them is usable during construction.

Parallel construction

The most recent publication in the area of parallel construction for BVH-trees dates back to 2013. Karras et al. [KA13] achieved significant speedup compared to early algorithms and made it possible to obtain a 90% ray tracing performance compared to off-line algorithms. Their work seems to be a giant leap towards using BVH for ray tracing in interactive applications.

Their algorithm is split into three phases: *processing*, *optimization* and *post-processing*. Additionally they add an optional phase zero which is *triangle splitting*.

Optional Phase 0: Triangle splitting

Since triangle splitting does not always add a performance gain it is only optional. To do so they make use of Ernst et al.'s [EG07] algorithm which constructs the AABB of each triangle and recursively splits them. Karras et al. introduced a heuristic that tries to overcome the problem of triangle splitting by only performing splits that improve the resulting performance. They first limit the amount of splits via

$$s_{max} = \lfloor \beta * m \rfloor \tag{3.2}$$

where m is the number of triangles in the scene and β is an adjustable parameter. The advantage of limiting the amount of splits lies in the predictability of memory usage. This limited amount of splits is then distributed throughout the triangles by calculating a priority p_t for every triangle t. Further they use a scale factor D and determine the number of splits for a triangle via $s_t = \lfloor D * p_t \rfloor$. The scale factor is chosen as large as possible so that it still satisfies $\sum s_t \leq s_{max}$.

When selecting split planes it is important that internal nodes near the root of the BVH-tree do not overlap. Therefore triangles that cross the split plane of the root node need to be split to increase the performance. This leads to the authors' conclusion of splitting every AABB which intersects the spatial median plane. They define the importance of split planes by how early it is considered during the construction of the initial BVH. This is examined by using two Morton codes for the minimum and maximum coordinates of the AABB and finding the highest differing bit.

Phase 1: Processing

The major part of this phase it to generate a BVH which is then further optimized in Phase 2. This is done by applying Karras' [Kar12] algorithm. The main part of this

[1] The two quality measures are *End-point overlap* (EPO) and *Leaf count variability* (LCV). These metrics describe the additional work used by nodes with overlapping bounding boxes and the standard deviation of the number of leaves intersected respectively.

algorithm is generating a binary radix tree which is then used for sorting the primitives according to the Morton codes of their center. In order to achieve this in a parallel fashion, they used a special layout which is described as follows: I and L are the sets of **I**nternal and **L**eaf nodes. I_0 is the root node. The left child node is located at I_γ or L_γ (in case of a leaf node) while the right child is at position $I_{\gamma+1}$ or $L_{\gamma+1}$ respectively. This layout offers the property that every internal node either has the same index as its first or last covered key. This holds for every inner node, since for its interval $[i, j]$ the children always cover $[i, \gamma]$ and $[\gamma + 1, j]$.

This means that the root node covers the range $[0, n-1]$ with the children containing $[0, \gamma]$ and $[\gamma + 1, n-1]$ respectively. The radix tree in Figure 3.6 illustrates this layout by horizontally aligning each internal node with the leaf it corresponds to. The split in the tree is always at the first differing bit. The horizontal bars show the range that is covered by the internal node.

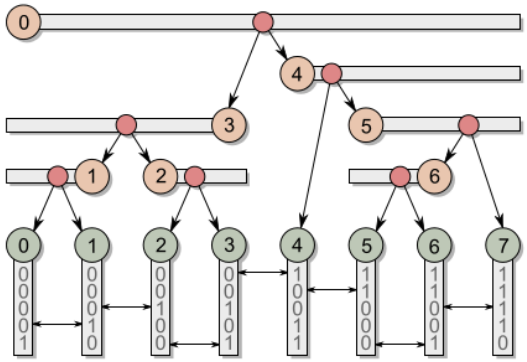

Figure 3.6: This radix tree (by Karass [Kar12]) has an index for every internal node, which corresponds to either the first leaf it covers or the last one. To visualize this, the internal nodes are aligned with they leaf the correspond to.

For the construction of a binary radix tree with this layout, it is necessary to find the keys covered by the internal nodes. Due to this layout it is trivial to obtain one end of an internal node's range. For obtaining the other end the following simple algorithm is used.

Every internal node I_i is processed in parallel. The first step is to find the direction d of the given node. This is done by evaluation the neighbors' keys k_{i-1} and k_{i+1}. The direction is either $+1$ for i being the beginning of the covered interval or -1 for its end. Moreover — through construction k_i and k_{i+d} belong to I_i and k_{i-d} belongs to I_i's sibling node I_{i-d}. Thus all keys belonging to I_i have the same prefix, but a different one to I_i's sibling's. Therefore the prefix can be bound by $\delta_{min} = \delta(i, i-d)$ with $\delta(i, j) > \delta_{min}$ for all keys k_j covered by I_i. This allows to choose d so that $\delta(i, i+d)$ corresponds to the larger one of $\delta(i, i-1)$ and $\delta(i, i+1)$.

The other end of the interval is then found by maximizing l so that $\delta(i, i+ld) > \delta_{min}$. This it done by iteratively trying powers of 2 until the condition $l_{max} > l$ is violated.

Via binary search in the range $[0, l_{max} - 1]$ the other end is found. Finally it is given by $j = i + ld$.

Therefore the length of I_i's prefix is obtained by $\delta(i, j)$ which is denoted as δ_{node}. With this information the split position γ can be obtained by applying binary search to maximize $s \in [0, l - 1]$ that satisfies $\delta(i, i + sd) > \delta_{node}$. Depending on the direction d of the node γ is either $i + sd$ in case of $d = +1$ or $i + sd - 1$ for $d = -1$. Now that i, j and γ are known, the children of I_i cover the ranges $[min(i, j), \gamma]$ and $[\gamma + 1, max(i, j)]$. Comparing the ends of the ranges respectively gives the information if the child is a leaf or not which is then referenced at node γ or $\gamma + 1$.

Our implementation of this procedure is shown in Section 5.1.1.

With the constructed radix tree the last step of generating a BVH-tree is done by assigning a bounding box for every internal node. Therefore a bottom-up traversal is used by starting one thread per leaf. At every internal node only the second arriving thread is allowed to process the node and pass through to its parent. The drawback of this is the $O(n)$ time complexity.

Phase 2: Optimization

In the topological optimization phase Karras et al. [KA13] minimize the SAH cost by so-called *treelet rotations*. A treelet is defined as a subtree of the BVH-tree with internal nodes of the BVH-tree being potential leaves of the treelet. First, a bottom-up traversal is done to determine a processing order of the nodes so that overlapping subtrees can not be processed simultaneously. For every node encountered during the traversal a treelet is formed with the node itself as root and a fixed number of descendants as treelet nodes and leaves. The treelet is then optimized by finding a corresponding binary tree that minimizes the SAH costs of the given treelet.

When forming a treelet it is better to maximize its SAH cost so that the reduction step has a higher potential. Therefore the treelet root and its children are taken in the first step. Further the treelet formation continues iteratively by turning the treelet leaf with the largest surface area into an internal node. Thus the leaf is removed from the set of leaves and its children are added to said set. This process goes on until the chosen amount of treelet leaves are in the set.

At this point a naive approach would consider every possible binary tree for a given treelet and select the one leading to the minimum SAH costs. This — obviously — inefficient solution is infeasible for a *fast* algorithm. Therefore several measures are taken to improve the efficiency of this procedure. First of all a predefined order to compute the binary trees' SAH costs is generated. Therefore a dynamic programming technique called *memoization* can be applied. Memoization is used whenever *small* sub results need to be calculated in order to obtain a bigger result. These sub results are stored — so-called *memoized* — in order to avoid recomputing them. In the case of treelet optimization memoization is applied to store the binary trees and their SAH costs. This way every possible binary tree is processed more efficiently.

Phase 3: Post-processing

In the post-processing phase the resulting BVH undergoes a simple transformation in order to be usable by a given traversal algorithm. In their case, Karras et al. [KA13], collapse certain subtrees to leaves with their triangles as linear list and transform the data so that Woop's [Woo04] intersection test can be used. Since this phase is dependent on the used traversal algorithm, we omit further details here.

3.3 Binary Space Partitioning

Another great acceleration data structure is the binary space partitioning tree. In contrary to the BVH described in Section 3.2 a BSP-Tree splits the scene arbitrarily in every level. Therefore a node in the resulting BSP-Tree does not contain a certain bounding box but the split plane which is used at it. The BSP-Tree therefore represents a fundamental concept in computer graphics: *binary space subdivision*. Although BSP is generally good for rendering purposes they are believed to be numerically unstable, infeasible to build and expensive to traverse. One of its advantages during buildup — the sheer possibilities for split planes at every level — is also the drawback that makes them costly to optimize.

The most common form of BSP used in practice is the k-d tree. k-d trees are a special form of BSP-Trees that only allow axis-aligned splitting planes. This obviously reduces the buildup time significantly as the number of possible splits diminishes drastically. Although k-d trees seem to be a promising alternative, we strongly believe that BSP-Trees can achieve better performance for real-time rendering. This belief stems from the fact that theoretically BSP has to outperform k-d trees when it comes to traversal.

Current-state BSP are not used in real-time rendering due to having a bad trade-off between build time and quality. Ize et al. [IWP08] showed that it is possible to use BSP-traversal for ray tracing in a competitive manner to k-d tree-traversal. While they have focused on the traversal algorithm itself and therefore constructed a BSP of higher quality, they still managed to limit the buildup complexity of the BSP-Tree to $O(n \log^2 n)$[2]. Although their ray tracing algorithm led to a reduction of triangle intersections by a factor 4, the higher traversal cost at each node reduces the speedup to 1.1 compared to the k-d tree. Through this they stated that it is either necessary to even further reduce triangle intersections or traversal costs to achieve a higher —and therefore significant — performance increase. Ize et al. have also not spent time on optimizing the buildup algorithm which therefore leads to an overall worse performance than a k-d tree based approach.

3.3.1 Construction Method

The construction of a high-quality binary space partitioning is believed to be an intractable problem. This comes from the fact that there is an ample amount of possible split planes

[2] k-d tree buildup is asymptotically bound by $O(n \log n)$

for every partition. Theoretically the quantity of these splits is infinite. This being said, Havran [Hav00] showed that for a k-d tree only splitting planes tangent to the clipped triangles are actually required. Therefore a k-d tree construction algorithm only has to consider 6 axis-aligned planes for every triangle which bounds the partition possibilities to $O(6n)$. Ize et al. [IWP08] explained that extending this reasoning would lead to $O(n^3)$ or even more split candidates for a general BSP, even this is an infeasible amount of investigation steps for every split. Therefore most construction procedures have used only a restricted pool of allowed split planes. Budge et al. [BCNJ08] introduced the — so-called — *restricted binary space partitioning*. Their approach only allows a small subset of possible plane normals on every split. This way they limit the complexity for the construction of a RBSP-Tree to $O(M^3 + MN \log N)$ where M is the number of allowed directions for split plane normals and N denotes the triangles in the scene. As already mentioned, a k-d tree — again — is a special case of the RBSP-Tree with the split planes restricted to the previously mentioned 6 planes.

The general construction algorithm for a BSP-Tree is roughly the same as common k-d tree building methods, with the only difference in the splitting phase. First the whole scene is taken and a split plane P_0 is chosen. This separates the scene into two partitions: *behind* P_0 and *in front of* P_0. In the next step the same procedure is applied in the two half-spaces. This is recursively done until no further splits are introduced. The stopping criteria can vary depending on the implementation but may be a fixed number of total splits, a certain heuristic that implies no improvement in further splits or just the simple fact that there is nothing to partition any further.

In case of the k-d tree, splitting does not take any planes but axis-aligned ones. Further during the construction of a k-d tree the process cycles through the axes so that — w.o.l.g. — first the x-axis is taken, then the y-axis and the z-axis afterwards. The cycle then restarts with the x-axis. We will display the BSP-Tree (and in fact the k-d tree) construction on a simple example.

Figure 3.7 shows a schematic example of a two-dimensional scene and the binary space partitioning applied to it. In Figure 3.7a we see a scene with several primitives and some split planes while Figure 3.7b displays the according BSP-Tree[3]. In this case the scene is first split along plane **0** and the root node is generated. The next recursive step is to take the partition *in front of* plane **0** in consideration. There the split plane **1a** is used. This leaves us with the two regions **A** and **B** which both cannot further be partitioned. The algorithm continues *behind* plane **0** where plane **1b** is used to split the scene. This also includes the problem of splitting a triangle. In this simple example the triangle is referenced in both subtrees instead of being split into two smaller ones. The subdivision *in front of* plane **1b** now contains only region **C**. Since this part of the scene solely contains the green circle and the reference to the early encountered triangle, a further split is not necessary. On the side *behind* plane **1b** there are still two primitives that can be split alongside another plane (plane **2**) leading to region **D** and **E**. Here the algorithm cannot further split the partitions and therefore comes to an end.

[3]Since this is a 2d-example and all splits are aligned with x- and y-axis it is also a k-d tree

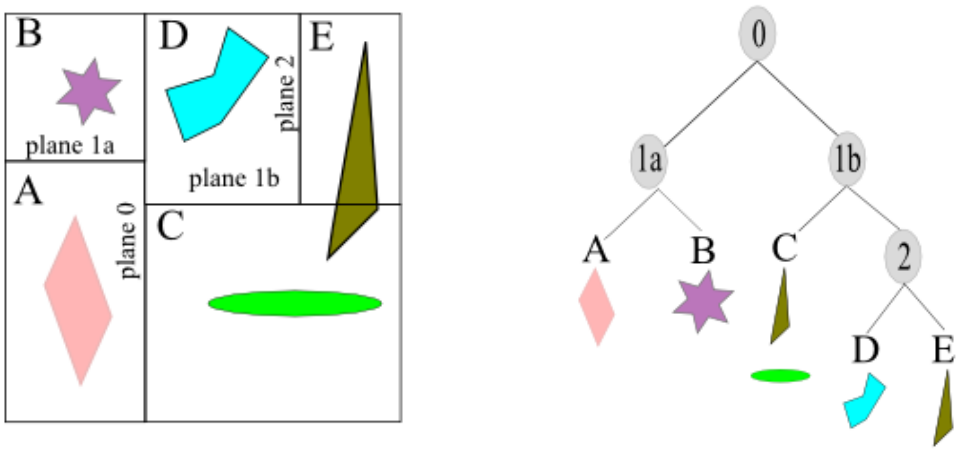

(a) Scene partitioned along several planes.

(b) Resulting BSP-Tree

Figure 3.7: A 2D example for a binary space partitioning (a) and the according BSP-Tree (b) [imgb]

3.3.2 Parallel Construction

We have not yet encountered any approaches of building a general binary space partitioning in parallel. This might be to due the fact, that a high quality BSP-Tree is believed to be intractable to generate. Further ray tracing seems to be the central topic of research in this area and it is dominated by k-d trees and BVH-trees. Although a BSP-Tree has the capabilities to outperform a k-d tree and a BVH-tree, it is still believed to end up with a building time that is too long. We believe that the restricted BSP [BCNJ08] would be a good candidate for parallel generation. Moreover k-d trees have already been constructed and traversed in parallel. The first implementation for parallel k-d trees was made by Zhou et al. [ZHWG08] in 2008. Since then the algorithm was finetuned by Wu et al. [WZL11b] including the SAH into the split plane selection. Recently Yang et al. [YYWX16] evolved the algorithm with ideas borrowed from octrees.

The first two approaches have in common that they try to leverage the GPU's resources by applying a breadth-first node generation for the first levels in parallel up to a certain point. This point is reached when there are enough child nodes to process each node in parallel. Figure 3.8 displays this design pattern. The green half of the image shows the upper levels where there are more processors than nodes per level. This allows to process multiple layers of the tree at the same time. Later when the number of nodes in every level surpasses the number of processors (purple part of the image) every node is processed simultaneously.

In the *multi-split k-d tree* approach of Yang et al. [YYWX16], they take a different route than showcased before. For their implementation they split every node on all three

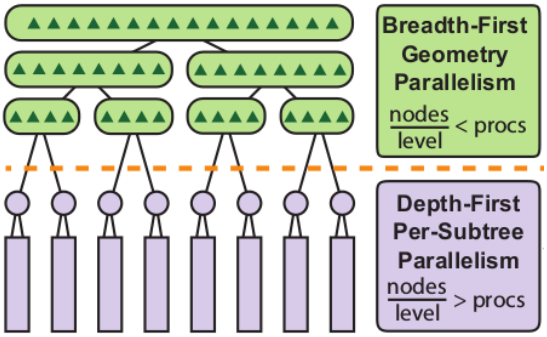

Figure 3.8: This image (taken from [CKL+10]) shows a pattern for generating the k-d tree in parallel. While in the upper levels (in green) multiple levels are constructed simultaneously, in the lower levels (purple) there are enough nodes per level to process these in parallel.

possible axes (x,y,z) and construct eight children. Then they examine every child with the surface area heuristic to find good split planes. They have also altered the traversal in order to fit with their data structure. With their approach they overcome the problem of slowly generating nodes in the upper levels through multiple splits and a width-first search. This uses the parallel opportunities of a GPU more efficiently and allows them to generate a higher quality k-d tree employing the SAH. As a result their tree ends up being shallower than normal k-d trees and contains less empty nodes. Through their traversal method they have also lowered the cost of traversal. Since the aim of this thesis is to develop an algorithm for general BSP-Tree construction, we will not go further into detail about k-d tree construction in this theoretical part.

3.4 Parallel Random-Access Machine.

True to this thesis' subject, parallelization, we will cover the Parallel Random-Access Machine (PRAM) model and its forms as well. The PRAM is an abstract machine which contains shared memory and mimics a parallel analogy of the Random-Access Machine(RAM)). As usual for theoretical abstract frameworks the PRAM omits problems like memory access, communication and synchronization. In contrary to the RAM it offers a number of processors which in turn can be used for modeling and analyzing the algorithms. The measure for algorithm costs is extended to two measures which are *time* **T** and *work* **W**[4].

3.4.1 Algorithmic Models

Since parallelism adds a new level of complexity to algorithmic design there are a few different models on how to describe those algorithms. We will just shortly cover two basic

[4]Work roughly describes **T** * number of processors

distinctions which are the *Single Instruction Multiple Data* (SIMD) and the *Multiple Instruction Multiple Data* (MIMD) model.

SIMD Model

The SIMD model describes a computing machine which offers multiple processors that all go through the same instruction set. This allow the exploitation of data parallelism but leaves out the usage of concurrency. Algorithm 3.1 shows a pseudo-code for the *tree summation* problem in the SIMD model[5].

The tree summation problem is defined as followed: Given an input array **A**, build the sum over all elements. The pseudocode in Algorithm 3.1 is run in parallel. Every processor $i, 0 \leq i < n$ executes the statements at the same time. In line 1 the value of A_i is stored in a local memory array of the same size in order to keep A unchanged. The lines 2 to 6 present the main work loop in which every processor sums up the according values. In the end — line 7 through 9 — processor 0 makes sure that the final output value is stored in s. Figure 3.9 shows the overall procedure whereas the number in each node shows which processor sums up its children.

Algorithm 3.1: SIMD tree summation [Träa]

Input: Array **A** of size $n = 2^h$
Output: $s = \sum_{0 \leq i < n} : A[i]$

```
1 B_i = A_i
2 for h ← 1 to h < n step h ← h * 2 do
3 |   if i < n/(2h) then
4 |   |   B_i ← B_2i + B_2i+1;
5 |   end
6 end
7 if i = 0 then
8 |   s ← B_i;
9 end
```

MIMD Model

The MIMD model extends the possibilities of the SIMD architecture by allowing processors to run different programs. This introduces another level of complexity into the PRAM system and allows for more sophisticated algorithm design. Main differences between MIMD and SIMD algorithms lie in the execution of forked programs with different instructions.

[5]This is just a naive algorithm to illustrate the SIMD model, there are far more sophisticated ones out there

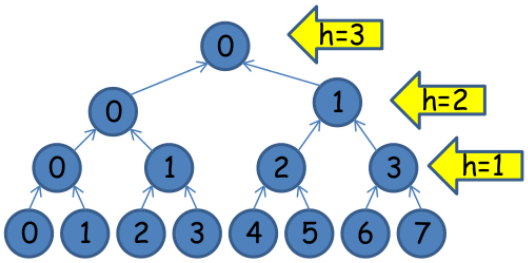

Figure 3.9: This image illustrates the tree summation process [Träa]

3.4.2 Read-Write Models

Through parallel execution and shared memory the problem of having read- and write-conflicts arise. In the theoretic model of PRAM there exist different models for dealing with these hindrances.

1. Exclusive read exclusive write (EREW)
   The EREW model allows only one process to read or write a single memory cell at the same time.

2. Concurrent read exclusive write (CREW)
   In the CREW model it is possible that multiple processors read the same memory in parallel, yet they are not allowed to write concurrently.

3. Exclusive read concurrent write (ERCW)
   This model was never really considered as useful since it does not offer any advantage over any of the other models, but adds more conflict potential.

4. Concurrent read concurrent write (CRCW)
   The mightiest model of the four is the CRCW. It allows any processor to access any memory cell at any time.

Since the CRCW model might lead to conflicts when writing, there are several strategies to deal with those conflicts. Amongst those design models for write-conflicts the most common ones are: *Common*, *Arbitrary* and *Priority*.

The Common model allows writes only when all processors write the same value and faults if that is not the case. The Arbitrary model makes only one processor's write go through and discards the others — all chosen arbitrarily. With the Priority strategy the processors are assigned a priority (e.g. by processor id) and the one with the highest priority is being the one that writes to the memory in the end.

As we will see in Chapter 4 the OpenCL framework allows to leverage the CRCW possibilities — i.e. concurrent writing and reading. Therefore we will not further go

into detail about the relationship about the read-write models since we will only need to consider the CRCW.

CHAPTER 4

OpenCL

4.1 Introduction

The OpenCL framework is an open, royalty-free standard which serves multiple platforms and offers the possibilities of parallel programming. It not only targets personal computers and systems, but also mobile devices, servers and embedded platforms. In this chapter we will explain how the OpenCL is structured and how we will make use of it, as well as give a short insight into its history.

4.2 History

Initiated by *Apple Inc.* OpenCL had its first release in August 2009 accompanying Mac OS X Snow Leopard as version 1.0. Originally the idea was a proposal in collaboration with technical teams of *AMD*, *IBM*, *Qualcomm*, *Intel* and *Nvidia*. It was then submitted to the Khronos Group which has been taking care of developing the OpenCL framework since then. The Khronos Compute Working Group was formed in June 2008, it contains representatives of CPU, GPU and embedded-processor manufacturers as well as software companies. The first technical specification for the OpenCL was publicly released on December 8th, 2008. Shortly after that, different vendors announced that they will add full support for the OpenCL to their toolkits.

Two years later, in June 2010 OpenCL 1.1 was approved by the Khronos Group. It included more functionality for parallel programming and performance. The following year the specification for OpenCL 1.1 was released with another set of features offering more possibilities to developers. Just two years later, in November 2013, OpenCL 2.0 was announced and technical specifications were released. Amongst its features, the most notable one was the Android driver extension, allowing Android devices to run OpenCL code. In November last year the specification for OpenCL 2.1 was released.

The latest version of the specification was released this year in March bearing the version 2.2.

4.3 Architecture

The OpenCL framework has a straight hierarchical architecture which we will describe briefly. The top-level API is written in the *C*, yet there are many wrappers available, making it accessible from other languages as well. With this API a *host* program is defined which is run on a CPU. From there it connects to multiple *computing devices* such as CPUs or GPUs. Each computing device consists of multiple *processing elements* which execute — so-called — *kernels*. Figure 4.1 displays the explained architectural model schematically.

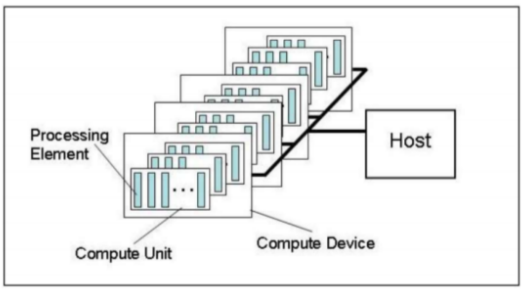

Figure 4.1: The architectural platform model of the OpenCL [TS12]

The aforementioned API offers possibilities to query for said computing devices and submit work to them. It further allows to control and manage the work queues and contexts. These work queues are used to submit kernels to computing devices while the context sums up a computation.

The earlier mentioned processing elements run kernels in parallel. This can be done in a data parallel fashion where a computing device is split in so-called working groups. Each of these groups then contains multiple work items. Figure 4.2 demonstrates this with a 2-dimensional grid structure.

Another important factor is the memory access. As global memory is expensive to access the OpenCL proposes a hierarchical memory structure which is shown in Figure 4.3. The hierarchy starts with the host device and its memory. It is connected to the compute device which often owns a global memory and in some cases constant memory. In order to make parallelism possible the compute device is split into work groups. Each of those containing its local memory and is split into several work items. The latter ones have their own private memory.

Another important part of the OpenCL architecture is its memory synchronization barriers. Roughly speaking it is possible to do synchronization between threads on every level. This means that within a work-group several work-items can use a memory fence in

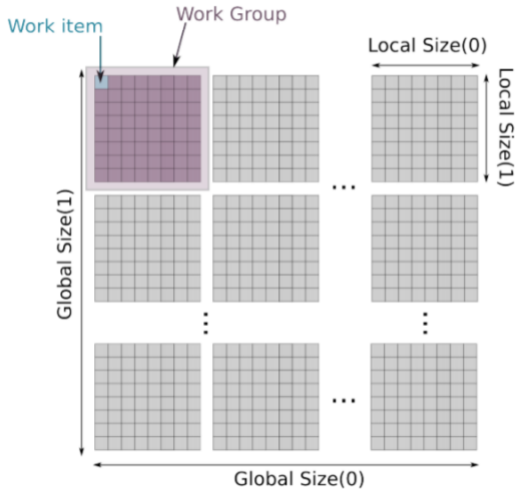

Figure 4.2: A 2-dimensional structure for execution [TS12]

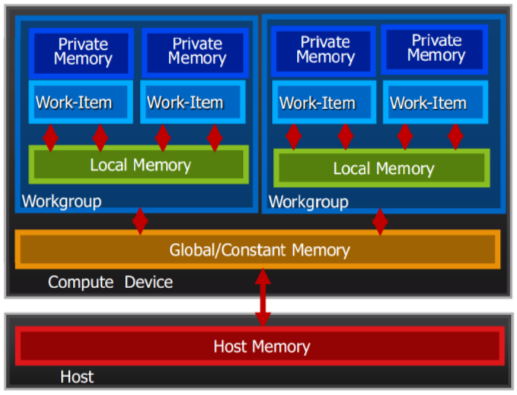

Figure 4.3: The memory hierarchy model of the OpenCL [TS12]

order to accomplish synchronization. On the next level, it is possible to do coarse-grained synchronization between work-groups.

The final level to consider is synchronous versus asynchronous execution models. In order to achieve this there exist different events which can be attached to items in the work queue. From the OpenCL API it is possible to either let every kernel start as soon as possible or to make kernels wait for each other. Figure 4.5 shows how this is made possible with event queues. The left side of the images displays concurrent execution whereas the right half demonstrates a sequential ordering.

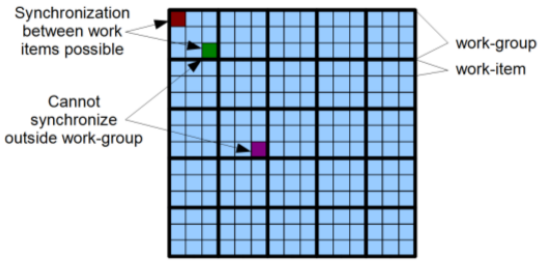

Figure 4.4: The memory synchronization withing the OpenCL framework [TS12]

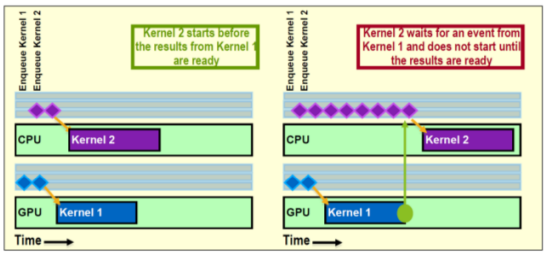

Figure 4.5: Execution control with OpenCL's event queue [TS12]

4.4 Code Example

Since we are not directly using the OpenCL C API in the implementation (see Section 4.5) we will give a short example of it here. This example is — for reasons of simplicity — just the basic matrix multiplication example. It is neither the best algorithm for this procedure, nor a special optimization. The idea behind this algorithm is that every thread takes row i of matrix A and the column j of matrix B. It then computes the element $C_{i,j}$. Through this we obtain the result of $C = A * B$. Algorithm 4.1 shows

Algorithm 4.1: Matrix multiplication

Input: Martix **A**, Matrix **B**
Output: $C = A * B$
1 **for** $i \in$ *rows of* A, $j \in$ *columns of* B **in parallel do**
2 $\quad C_{i,j} \leftarrow i \cdot j$
3 **end**

the pseudocode of the algorithm while Figure 4.6 shows the OpenCL kernel. At first we define a kernel for the matrix multiplication with pointer to the matrices A, B and C as input. Additionally we add the number of rows of the input matrices since we have to deal with decay of pointer. In line 7 and 8 we retrieve the thread id on the 2-dimensional grid. We use these ids as indices i and j for selecting the row and column vectors for the

```
1  __kernel void matrixMultiplication(
2    __global int* A,
3    __global int* B
4    __global int* C,
5    int rowsA, int rowsB)
6    {
7      int i = get_global_id(0); //2D-Thread-Id in first dimension
8      int j = get_global_id(1); //2D-Thread-Id in second dimension
9
10     //dot product
11     int sum = 0;
12     for (int k = 0; k < rowsA; k++)
13     {
14         sum += A[j*rowsA+k] * B[k*rowsB+i];
15     }
16
17     //right back the result
18     C[j*rowsA+i] = sum;
19   }
```

Figure 4.6: Matrix multiplication kernel with OpenCL

dot product. The loop in line 12 is used to calculate the dot product. Finally in row 18 the value for $C_{i,j}$ is written into the right memory cell.

4.5 Usage

In this thesis we will use the OpenCL framework via a F# wrapper. This allows us to use the functionality directly from the projects which are developed with C# and F#. It also allows a more structured layout of the code and a direct API for usage.

The F# to OpenCL compiler is based on so-called *Quoted Expressions* which are a part of the *Code Quotations* feature of F#. This language feature offers the possibility to generate an abstract syntax tree as representation of F# code. With this tree it is possible to alter or generate code in any given language, hence we are using it for our purpose.

Our cross compiler is the work of Georg Haaser and is still a work in progress as of the time of writing this thesis.

4.5.1 Matrix Multiplication Example

To present the way the code in chapter 5 will be laid out, we are making use of the formerly shown matrix multiplication example.

As we can see in Figure 4.7 the program pretty much looks the same. The following algorithm (shown in Figure 4.8) shows how we compile and call the kernel from a top

```
1  let matrixMultKernel
2      (A: buffer<int>)
3      (B: buffer<int>)
4      (C: buffer<int>)
5      (rowsA: int)
6      (rowsB: int) =
7      kernel {
8          let i = get_global_id(0) //2D-Thread-Id in first
               dimension
9          let j = get_global_id(1) //2D-Thread-Id in second
               dimension
10
11         //dot product
12         let mutable sum = 0
13         let mutable k = 0
14         while k < rowsA
15                 sum <- sum + A.[j*rowsA+k] * B.[k*rowsB+i]
16                 k <- k + 1
17
18         //right back the result
19         C.[j*rowsA+i] <- sum
20     }
```

Figure 4.7: Matrix multiplication kernel with F# and OpenCL

level function. First we store the size of matrix A in variable, then create the three needed buffers. In line 14 the kernel is compiled by some magic. Three lines down — in line 17 — the kernel is called. We first provide the number of global threads and the group size. The other parameters are the buffers and the number of rows of the input matrices. After the kernel is run we create the output array C in line 20. In line 23 we finally download the values from the buffer into the array and return the latter in the last line.

```
let matrixmultiplication
    (ctx: OpenClContext)
    (A: int[])
    (B: int[])
    (rowsA: int)
    (rowsB: int) : int[] =

        let sizeA = A.Count

        //create the buffers
        let bufferA = ctx.CreateBuffer A :> buffer<_>
        let bufferB = ctx.CreateBuffer B :> buffer<_>
        let bufferC = ctx.CreateBuffer (Array.CreateZero sizeA)

        //compile the kernel
        let compiled = compileKernel ctx matrixMultKernel

        //call the kernel
        compiled sizeA sizeA bufferA bufferB rowsA rowsB
           bufferC

        //create outputArray
        let C : int[] = Array.CreateZero sizeA

        //download the values from the buffer
        bufferC.Download(C)

        //return the result
        C
```

Figure 4.8: Compilation and call of the kernel

CHAPTER 5

Implementation

This chapter will deal with the implementation detail of the thesis. Throughout the implementation of the discussed data structures we came across certain road blocks and came to a realization that changed the planned implementation. In this place we are going to describe the thought process and development of the final data structure and algorithms.

We will mostly focus on the algorithms themselves. First we will describe the implementation of the bounding volume hierarchy. Then we will show the problem that arose for our usage scenario.

The second part of this chapter displays our take on parallelizing the binary space partitioning and incorporating it into the BVH. This will be followed by demonstrating another complication that occurred.

The third part gives insight into our solution for the aforementioned problems by combining a grid with the BSP.

The use cases we had in mind for said data structures were culling queries[1] for the BVH and sorting queries[2] for the BSP.

5.1 Bounding Volume Hierarchy

The first part of the implementation focuses on the bounding volume hierarchy. As already mentioned in Section 3.2.1 we planned on implementing Karras et al. [LGS+09] construction method. While they used the CUDA framework we used the OpenCL framework within our F# ecosystem.

[1] Frustum culling, see Section 1.1.2
[2] Transparency sorting, see Section 1.1.3

The first step in the implementation was to reproduce Karras' [Kar12] algorithm for parallel construction, his will be shown in Section 5.1.1. We further planned on implementing the second step *treelet optimization*, followed by *early triangle splitting* as explained in Section 3.3.2.

5.1.1 BVH Construction

The top-level function to build the BVH-tree is shown in Figure 5.1. First we create the necessary arrays to store the leaves and the nodes during the parallel run on the GPU. We then generate the morton code for each Leaf and sort them. Then we prepare the data for the BVH-tree construction. With the call to ***constructInternalNodes***, which is the compiled version of ***constructInternalNodesKernel*** we build the BVH-tree. In the last line we put together the resulting data in a simple struct.

Since it is not possible to link to different data structures within the structs for the internal nodes we save the id of the child and parent nodes. To do so, our implementation stores the ids within the nodes with a shift for leaves. While internal nodes have the id range from 0 (root) to $n-1$ (rightmost internal node), leaves take up the negatives numbers. Leaf 0 therefore has the id -1, while the leaf $n-1$ has the id $-n$. This way we can distinguish between internal nodes and leaves during operations.

The tree layout is designed according to Karras [Kar12] as shown in Section 3.2.1.

Figure 5.2 shows the kernel of the core function for the creation of the BVH-tree. First we obtain the id of the thread, leading to two interesting parts of the algorithm. ***determineRange*** finds the range that is covered by the internal node given by the id. After obtaining this range we determine the split position with the ***findSplit*** function. Having found the range and the split position, we can link the nodes to each other(line 18 to 40)[3].

To determine the range we are using binary search on the sorted Morton codes. In Figure 5.3 we see the function used to find the covered range for every internal node. First we check if we have the root node in which case we return the full range.

We first make use of the ***delta*** function to determine the direction of this node. Said function returns the length of the common prefix for the Morton codes on positions given by the first two arguments. In line 9 to 12 we calculate an upper bound for the size of the range. With this upper bound we start a binary search to find the other end of the range. The final range is given by the node's (also thread's) id and the result of the calculation in line 21. The last line ensures that the range is always in the for (i, j) with $i < j$.

The ***findSplit*** function works roughly the same way as the ***determineRange*** function. A binary search is used to find highest differing bit in the Morton codes within the two ends of a node's range.

[3]For this we defined the operator (<==) in order to be able to directly write to a memory location.

BVH-tree building method

```
1  member x.Build(data : Leaf[]) =
2      let numObj = data.Length
3      let (gloablSize, workGroupSize) = getWorkSizes numObj
           groupSize
4
5      let mortoncodes = ctx.CreateBuffer (Array.zeroCreate numObj
           : uint32[]) :> buffer<_>
6      let leaves = ctx.CreateBuffer (data |> Array.map (fun x ->
           x.BoundingBox)) :> buffer<_>
7
8      //find morton codes
9      findMortonCode gloablSize workGroupSize leaves mortoncodes
           numObj
10
11     //sort
12     let sortedObjIds = ctx.CreateBuffer (Array.zeroCreate
           numObj : int[]) :> buffer<_>
13     let indices = tools.CreatePermutationSort (mortoncodes)
14     tools.CompactWithIndex(indices, mortoncodes, sortedObjIds)
           |> ignore
15
16     //build the tree
17     assignObjectID gloablSize workGroupSize leaves sortedObjIds
           objects numObj
18     let nodes = ctx.CreateBuffer<MyNode>(int64 numObjects - 1L)
           :> buffer<_>
19     constructInternalNodes gloablSize workGroupSize objects
           nodes mortoncodes numObj
20
21     createBVH nodes leaves
```

Figure 5.1: The top-level BVH building method of the `BVHBuilder`. The `BVHBuilder` stores the `OpenClContext` **ctx** as well as **tools** of type `OpenClTools`, which offer various algorithms

Kernel ***constructInternalNodeKernel***

```
let constructInternalNodeKernel
    (leafNodes: buffer<Leaf>)
    (internalNodes : buffer<MyNode>)
    (sortedMortonCodes : buffer<uint32>)
    (numObjects : int) =
    kernel {
        let id = get_global_id(0)
        if id < (numObjects-1) then
            // Find out which range of objects the node
               corresponds to.
            let (firstx, lastx) = determineRange
               sortedMortonCodes numObjects id

            let first = if firstx < 0 then 0 else firstx
            let last = if lastx >= numObjects then numObjects-1
                else lastx

            // Determine where to split the range.
            let split = findSplit sortedMortonCodes first last

            let indexA = split
            let indexB = split +  1

            // leaves are negative / inners positive
            let valueA = if split = first then getLeafId indexA
                else getNodeId indexA
            let valueB = if split + 1 = last then getLeafId
               indexB else getNodeId indexB

            // Record parent-child relationships.
            if split <> first then
                internalNodes.[indexA].Parent <== id
            else
                leafNodes.[indexA].Parent <== id

            if split + 1 <> last then
                internalNodes.[indexB].Parent <== id
            else
                leafNodes.[indexB].Parent <== id

            let myId = getNodeId id
            internalNodes.[myId].Left <== valueA
            internalNodes.[myId].Right <== valueB
            internalNodes.[myId].First <== first
            internalNodes.[myId].Last <== last
            internalNodes.[myId].Split <== split
            internalNodes.[myId].ID <== id
    }
```

Figure 5.2: Kernel of the core function for BVH construction

Function ***determineRange***

```
1  let determineRange (mortonCodes : buffer<uint32>) (numObjects :
       int) (id : int) =
2      if id = 0 then
3          (0, numObjects-1)
4      else
5          //  Determine direction of the range (+1 or -1)
6          let direction = sign (delta id (id+1) numObjects
               mortonCodes - delta id (id-1) numObjects mortonCodes
               )
7
8          // Compute upper bound for the length of the range
9          let deltaMin = delta id (id - direction) numObjects
               mortonCodes
10         let mutable lMax = 2
11         while delta id (id + lMax * direction) numObjects
               mortonCodes > deltaMin do
12             lMax <- 2 * lMax
13
14         // Find the other end using binary search
15         let mutable l = 0
16         let mutable t = lMax / 2
17         while t >= 1 do
18             if delta id (id + (l + t) * direction) numObjects
                   mortonCodes > deltaMin then
19                 l <- l + t
20             t <- t / 2
21         let j = id + l*direction
22
23         if direction < 0 then (j,id) else (id,j)
```

Figure 5.3: Function to determine the range of an internal node

5.1.2 Treelet Optimization & Triangle Splitting

After the BVH-tree has been generated by the shown algorithm the optimization phase would begin. In order to optimize the structure of the BVH-tree every node needs its associated SAH. As Karras et al. [Kar12, LGS+09] have shown, the best way to do this is a parallel bottom-up traversal. They started a thread for every leaf in the tree and followed the parent pointer. Whenever a thread encounters an internal node it increments an internal counter and — if the counter is 0 — terminates. The second thread arriving at each internal node is the one that processes it. Karras [Kar12] used this method to calculate the bounding boxes for every node while later Karras et al. [KA13] did the same for SAH calculation as well as treelet generation and optimization.

During the implementation of said optimization and bottom-up traversal we realized that we are, in fact, starting a thread for every leaf in order to calculated the needed data — bounding boxes — for our culling queries. Therefore instead of using these threads for traversing the BVH-tree we could already use them for evaluating every leaf with the actual query. This results in work of $O(n)$ and time of $O(1)$. Although a traversal of the final tree would lead to — theoretical — work of $O(\log n)$ we still would have to write and compact an array with visibility flags for every leaf node. Therefore we would again end up doing $O(n)$ work and thus lose the advantage of using the BVH-tree.

After some consideration we also came to the result that even a parallel traversal can not improve this situation. This stems from the fact that classical parallel traversal — mostly used for ray tracing — is used for doing multiple traversals at the same time. Frustum culling — on the other hand — is only *one* query per scene leading to one traversal. In order to parallelize this, a synchronized data structure (e.g. a stack or queue) would be needed.

After reconsideration of bounding volume hierarchy in our scenario we omitted the optimization since it is unnecessary in our use case.

5.2 Binary Space Partitioning

As already explained in the theory part of this thesis (see Section 3.3) constructing an optimal BSP is believed to be an NP-Hard problem. Our first idea to parallelize the BSP-Tree construction was to gradually decrease split planes evaluated per tree depth according to a-thread-to-nodes ratio. This approach would be similar to Budge et al.'s[BCNJ08].

At this point of the implementation we already had implemented the BVH and thought about combining it with the BSP. Through some discussion the idea arose that we could use the BVH to split the scene into small sets and build a BSP-Tree for each of these sets.

Due to the construction algorithm of the BVH-tree, fortunately it has the nice property that every internal node contains information about the range of leaves it covers. We

therefore though of an early exit during the construction to obtain small sets of leaves. This would leave us with a fast way to separate the scene and tiny instance for the harder problem of generating a BSP-Tree.

The necessary full BSP-Tree construction within a single kernel leads to limitations such as no recursive functions and no dynamic memory allocation. This implies the need for a stackless construction. In order to use all those small BSP-Trees for transparency sorting, a kernel handling this scenario was necessary as well. In the following sections (Section 5.2.1 construction and Section 5.2.2 traversal) we show how we implemented those two kernels.

5.2.1 BSP-Tree Construction

Before going into detail about how we create the tree, we will give a short overview of the algorithm. Our BSP-Tree construction algorithm takes a triangle and generates a split plane from it. This is simply done by taking the cross product of two edges as plane normal and the connecting point. After obtaining said plane, the triangles are evaluated and separated into four groups: *same*, *front*, *back* and *split*. The first set consists of the triangles that lie completely on the selected split plane. The following two consist of the triangles that lie entirely on one side (front and back respectively[4]) of the split plane. The last group of triangles are those that go through the plane and therefore need to be split.

The split of triangles leads to three new triangles. Figure 5.4 shows this procedure. In the first image Figure 5.4a we see the triangle that needs to be split. The result of is shown in Figure 5.4a.

After splitting of the original triangle, each of the resulting triangles can be classified to either belonging to the front or back group.

After having classified every triangle, and splitting when necessary, we are left with the three sets: *same*, *front* and *back*. At this point a node is created with the information about the split plane and a list of all the triangles in the *same* set.

The next step is to find out the root nodes for the next level in the BSP-Tree which are then used as left (front) and right (back) children of the created node. For this we take a simple heuristic that checks every node in the next level and counts the number of splits. In the end we take the node with the least split for its respective subtree. This is the point were the left and right subtree would be generated in a recursive fashion. This is done until there are no triangles left.

Building in a kernel

In order to fit the showcased algorithm into a kernel, we had to get rid of recursions. We further are not allowed to dynamically allocate memory, which leaves us with a buffer of

[4]Since we do not have a certain view point here, front and back are defined via positive and negative distance to the plane respectively

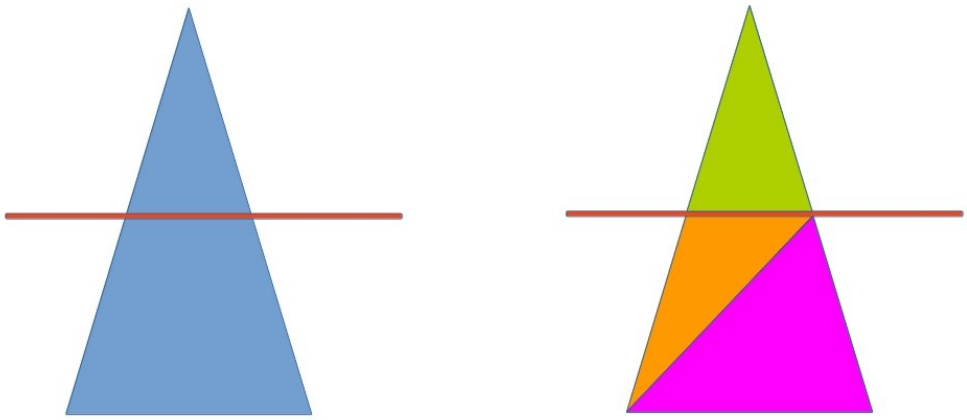

(a) Triangle to be split (b) Resulting triangles

Figure 5.4: These images show a triangle that is split (a) by a plane resulting in three triangles (b)

"empty" nodes that need to be filled. To overcome the limitations our node is defined as demonstrated in Figure 5.5. First we have the node information such as the split plane, its children (**Left** and **Right**) as well as the parent id. The field **Same** stores the id of the next node in the same "list" or -1 if there is none, to simulate simulate a linked list. The **Leaf** stores the leaf information holding a triangle. The field **ID** is used for identification and **Original** stores a back reference to the original triangle after splitting it.

The last two fields are used for building and traversal. With **Level** we store information about which level the node is located at. Instead of using recursion during the build and traversal, it is increased; and decreased once we reach a leaf node (i.e. one that is alone on its level). The field **LoR** is used to store information about the aforementioned groups to which the triangle belongs. With this information and the level we fully can simulate the recursion within a loop. For this we need the enumeration type `LeftOrRight` which has the enumerals `LEFT`, `RIGHT`, `SPLIT`, `NONE` (as start value) and `DONE` (to indicate a node that is finished).

Figure 5.6 shows how we build the BSP-Tree. Since we are doing this in parallel for multiple sets of triangles, we first need to know in which set we operate. For this we use the information stored in the **cells**[5]. Once we have obtained said information we initialize the nodes as "empty" in the *initialization loop*. Next we define certain variables that are needed for the construction.

After the *initialization loop* we set the needed variables before the main loop starts. Here we first obtain the current **rootNode**. This node is used to classify the triangles on the

[5]See Section 5.2.4 for the `Cell` struct definition and why we it this here

BSPNode struct definition

```
1   type BSPNode =
2       struct
3           val mutable public Splitplane       : Plane
4           val mutable public Left             : int
5           val mutable public Right            : int
6           val mutable public Parent           : int
7           val mutable public Same             : int
8           val mutable public TriangleId       : int
9
10          val mutable public ID               : int
11          val mutable public Original         : int
12          val mutable public Level            : int
13          val mutable public LoR              : LeftOrRight
14      end
```

Figure 5.5: Definition of BSPNode

current level (**curLevel**). If **curLevel** is greater than the level of the **rootNode** we still have the same root node as in the last level. This can only happen if said node does not have any other triangles on its level and its side. *Note:* this would be the *base case* of a recursive algorithm. We therefore need to backtrack the level to find out where we have to continue. This is done in *backtrack loop*. Here we reduce the **curLevel** and backtrack to the node's parent. If there is a parent (i.e. we are not the BSP-Tree's topmost root) we check if we have to traverse the right subtree. *Note:* this would be the second recursive call. In case both subtrees are already done, we set the status of this node to `DONE` and go to its parent.

After backtracking the **curLevel** and setting the correct **rootId** we continue by creating the split plane. In *evaluation loop* we evaluate all the other triangles of the cell.

For every node in this cell we check if it is in the current level and on the same side as the root triangle. *Note:* essentially, we check if the triangle is in the correct list for the given node. The node's corresponding triangles are then further classified. In order to do so we obtain the **signs** from the function ***frontBackCheck*** (see Section 5.2.1). Through this we can classify the triangle to one of the earlier mentioned four groups. If the triangle lies on the current split plane, all of the vectors from its points to the plane's point are orthogonal to the plane's normal and the dot products yield zero. In this case we traverse the simulated **Same**-list and append the current node to the end of it and set its status to `DONE`. If **signs** is either all positive or all negative we set the status of the node to `LEFT` or `RIGHT` respectively.

Kernel ***buildBSPKernel***

```
let buildBSPkernel (cells : buffer<Cell>) (leaves : buffer<Leaf>) (bspNodes : buffer<BSPNode>) (numLeaves: int) (epsilon : float32) =
  kernel {
      let id = get_global_id(0)
      let extra = 5 //multiplier for buffer calculations
      if id < cells.Count then
          ###run variables initialization###
          let cell = cells.[id]

          //create BSP Leaves
          let mutable k = nodeBufferStart
          let mutable vIndex = vertexStartOffset
          for k = nodeBufferStart to nodeBufferStart + numNodes - 1
              ###initialization loop###

          let mutable run = 1

          while run = 1 do
              //take leave
              let mutable rootNode = bspNodes.[rootId]
              //if we got a root from last level, we finished this subtree in the last level and we have to roll back
              while run = 1 && rootNode.Level < curLevel do
                  ###backtrack loop###

              rootNode <- bspNodes.[rootId]
              let curId = rootId
              let splitPlane = findSplitPlane
                  leaves.[bspNodes.[curId].TriangleId]
                  leaves.[bspNodes.[curId].TriangleId+1]
                  leaves.[bspNodes.[curId].TriangleId+2
              rootNode.Splitplane <- splitPlane
              let mutable i = nodeBufferStart
              let loopMax = curFreeId

              while run = 1 && i < loopMax do
                  ###evaluation loop###

              if run = 1 then
                  ###next level preparation###

              curLevel <- curLevel + 1
      }
```

Figure 5.6: Kernel for building the BSP-Tree

Evaluation loop of ***buildBSPKernel***

```
while run = 1 && i < loopMax do
   ###evaluation loop###
    if i <> curId then
        //check front or back
        let mutable node = bspNodes.[i]
        //check if the leaf with id i is at the current level
           and current side, if so work with it
        if node.LoR = curLoR && node.Level = curLevel then
            let p0 = leaves.[node.TriangleId]
            let p1 = leaves.[node.TriangleId+1]
            let p2 = leaves.[node.TriangleId+2]
            let signs = frontBackCheck splitPlane p0 p1 p2
               epsilon

            //set leaf's properties
            node.Level <- curLevel + 1

            if signs = Signs.ZERO then
                node.LoR <- LeftOrRight.DONE
                node.Level <- curLevel
                ###add to same list###
            elif (signs &&& Signs.NEG) = Signs.NONE then
                node.LoR <- LeftOrRight.LEFT
            elif (signs &&& Signs.POS) = Signs.NONE then
                node.LoR <- LeftOrRight.RIGHT
            else
            //split
                node.LoR <- LeftOrRight.SPLIT
                let (n0, n1, n2) = splitTriangle node leaves
                   splitPlane vIndex
                //left and right already set in the function

                //add the three nodes at the end of the buffer
                curN.ID <- curFreeId
                bspNodes.[curFreeId+0] <- n0
                bspNodes.[curFreeId+1] <- n1
                bspNodes.[curFreeId+2] <- n2
                curFreeId <- curFreeId + 3

   bspNodes.[i] <- node
   i <- i + 1
```

Figure 5.7: Evaluation loop of the kernel

Next level preparation of ***buildBSPKernel***'s main loop

```
1  if run = 1 then
2      ###next level preparation###
3      //findRootnodes
4      let bestIDLeft = findBestSplit bspNodes leaves
          nodeBufferStart curFreeId (curLevel+1) LeftOrRight.LEFT
          epsilon
5      let bestIDRight = findBestSplit bspNodes leaves
          nodeBufferStart curFreeId (curLevel+1) LeftOrRight.RIGHT
           epsilon
6
7      //set this nodes' properties
8      rootNode.Left <- bestIDLeft
9      rootNode.Right <- bestIDRight
10     rootNode.LoR <- LeftOrRight.DONE
11     bspNodes.[curId] <- rootNode
12     if bestIDLeft > 0 then
13         bspNodes.[bestIDLeft].Parent <== curId
14         curLoR <- LeftOrRight.LEFT
15         rootId <- bestIDLeft
16
17     if bestIDRight > 0 then
18         bspNodes.[bestIDRight].Parent <== curId
19         if bestIDLeft < 0 then
20             curLoR <- LeftOrRight.RIGHT
21             rootId <- bestIDRight
22
23     curLevel <- curLevel + 1
```

Figure 5.8: Next level preparation section of the kernel

All the other cases mean that the triangle has points of either side of the split plane. Therefore we need to split the triangle as explained in Section 5.2.1. To do so we call the method ***splitTriangle*** (described in Section 5.2.1) which leaves us with 3 new nodes. Through **curFreeId** we keep track of the next free index in the node buffer we are working with and store the leaves there. *Note:* this simulates an add to the global triangle list. Finally we write the changes to the current node.

After iterating through and classifying all the nodes we are left with deciding on how to continue in the next level. In *next level preparation* we do exactly that. First we find the root nodes of the left and right subtrees with the simple heuristic explained in Section 5.2.1. This is done via the ***findBestSplit*** function (also shown later in this section). The result of those selections are stored as left and right children of the current root node. If there are no children on one side, ***findBestSplit*** returns -1 to identify an empty subtree. In case there exist children on the left side we set **curLoR** — showing the current side of the tree — to `LEFT` and updating the **rootId**. *Note:* This simulates the recursive call for the left subtree. If the left subtree is empty, we set **curLoR** to `RIGHT` to continue in the right subtree. In any case we store the parent pointer in both child nodes.

Finally we increase **curLevel**.

Used functions

In this subsection we shortly explain the function used during the construction. The ***frontBackCheck*** function evaluates where the points of the triangles lie compared to the plane. To do so it evaluates the dot product of the normal and the line from each point to the plane's point. Then it calls ***aggregateSigns*** which does a simple check for positive and negative values and combines them in a bit mask. In ***findBestsplit*** we do a quadratic loop through all the leaves to see which are on the same side and level. For each of those triangles we count how many of the others it would split[6]. In the end we return the id of the one with the lowest amount of splits. With the ***splitTriangle*** function we start a point of the triangle and follow the edge to the next one. We first add the start point to a the positive or negative list[7], depending on which side of the plane it lies. Along the edge we either stay on the same side or cross the split plane. If we do not cross the plane we add the next point to the same list and continue following the next edge. The other case leaves us with a point where the plane cuts through the triangle. This point is added to both of the lists and the end point of the edge is added onto the negative or positive list respectively.

After following every edge we are left with two lists, one containing 3 points and one with 4 (top and bottom half of Figure 5.9 respectively). Now we go through each of the lists and take three points to construct a triangle. The list with 3 entries will trivially result in a single triangle (**A**,**D** and **E** in Figure 5.9). The other list contains the 4 points

[6] We ditched this part of the implementation as explained in Section 6.2

[7] in our case a fixed size array, this is possible since there are no more than 4 points per side

B, **C**, **D**, **E** of Figure 5.9. Due to construction this algorithm already "sorts" the points accordingly. If we start with edge **BA**, we first add point **B** followed by **D**, **E** and lastly **C**. This results in the two triangles shown in the figure. Other possibilities are **BC** (B,C,E,D), **AB** (D,B,C,E) and **CA** (C,E,D,B). We always use the points 1 to 3 for the first triangle and 2 to 4 for the second. This way the first two possibilities (**BA**, **BC**) result in the shown triangles while the other two (**AB**, **CA**) would yield the triangles **BCD** and **CDE**.

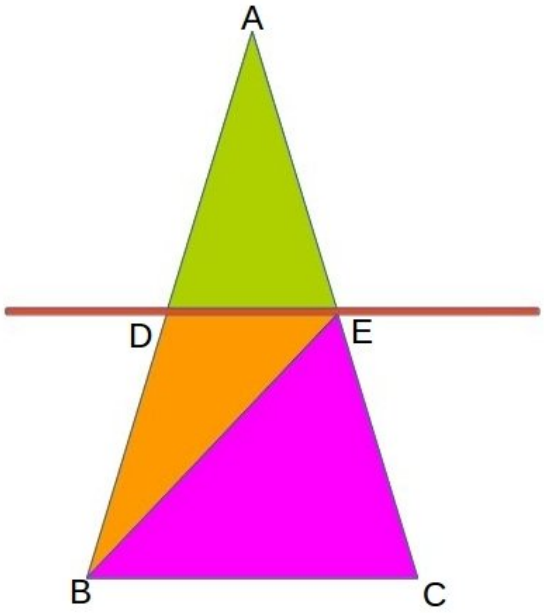

Figure 5.9: These images shows the points created during the split

During the split we also set the side (**LoR**) of the nodes and finally return them

5.2.2 BSP-Tree Traversal

In this section we will outline the simple traversal algorithm as well as how we — once more — implemented it within the OpenCL restriction for kernels.

The traversal in our case is a sorting query with an eye point and either a *front-to-back* or a *back-to-front* order. We start at the root node and evaluate whether the eye point is in front or back of the split plane[8]. Then we recurse into the respective child tree and continue in recursive fashion until we reach a leaf node. This leaf is then added to the output list and we backtrack to its parent. The latter one is then added to the output list and the recursion is continued in its other child-tree. This in-order traversal results in a sorted list for the given eye point.

[8]The sort order is simply a change of sign here

Kernel ***sortBSPTreeKernel***

```
let sortKernel (eye: V4f) (cells: buffer<Cell>) (nodes : buffer
   <BSPNode>) (outArray : buffer<int>) (cellStartEnd: buffer<
   int>) =
    kernel {
        let id = get_global_id(0)
        //let extra = 5

        if id < cells.Count then
            let cell = cells.[id]
            let firstNodeOffset = cell.FirstIndex / 3
            let lastNodeIndex = cell.LastIndex / 3 //end of
               buffer
            //prepareNodes
            for k = firstNodeOffset to lastNodeIndex do
            nodes.[k].LoR <== LeftOrRight.NONE

            let mutable run = 1
            while run = 1 do
                //take node
                curNode <- nodes.[curID]
                let left = curNode.Left
                let right = curNode.Right
                if left < 0 && right < 0 then
                    //we reached a leaf of the tree -> add it
                       to the output array
                    ###follow same-pointer###
                else
                    ###Internal node###
                if curID < 0 then run <- 0

    }
```

Figure 5.10: Kernel for traversing the BSP-Tree

Internal node part of ***sortBSPTreeKernel***

```
1  ###Internal node###
2  if curNode.LoR = NONE then
3      //we are at a new node
4      let height = V4f.Dot(splitplane.Normal,
5                           (eye - splitplane.Point))
6      if height > 0.0f then
7          if left > 0 then
8              curNode.LoR <- LEFT
9              curID <- curNode.Left
10                     else
11 //no left child, add node to resultlist and traverse right
12             ###follow same-pointer###
13         curNode.LoR <- DONE
14         if right > 0 then //traverse right
15             curID <- curNode.Right
16         else //we are done, backtrack
17             curID <- curNode.Parent
18
19     //traverse back
20     if not (height > 0.0f) then
21         //same as left but with LEFT and RIGHT switched
22     elif curNode.LoR = LEFT then
23         if nodes.[left].LoR = DONE then
24             ###follow same-pointer###
25             //left child is done, go into right child
26         curNode.LoR <- DONE
27         if right > 0 then
28             curID <- curNode.Right
29         else
30             //if there is no right child, we are done
31             curID <- curNode.Parent
32     elif curNode.LoR = RIGHT then //same as left, but switched
33     elif curNode.LoR = DONE then
34         //we are done with internal node update curID to parent
35         curID <- curNode.Parent
36
37     nodes.[curNode.ID] <- curNode
38     if curID = -1 && curNode.LoR = DONE then run <- 0
```

Figure 5.11: Kernel for traversing the BSP-Tree

To fit this algorithm into a kernel, we — again — have to deal with the limitations explained in the beginning of Section 5.2.1. In order to achieve this we use the same *workaround* as already shown in Section 5.2.1. Figure 5.10 shows the traversal. After identifying the correct range in the global buffer we first set every node's **LoR** to `NONE`. In the *main loop* we first check if we are currently dealing with a leaf. In this case we add it to the output list and traverse the simulated **Same**-list. Via a **counter** we keep track of where in the output buffer we are storing the current entries. We further backtrack to the leaf's parent. *Note:* this would be the base case of a recursive algorithm

If we are working on a node we identify the current stage via the node's **LoR**. The first case is a — so far — unseen node. Here we first check on which side of the split plane the eye point is, and then set the **LoR** to the side we are going to traverse. In case there is no child on this side, we again add the **Same**-List to the output and set the traversal to `DONE`.

In case the working node has its **LoR** set, we know we have to traverse the respective subtree. If this subtree is done, we add the current node and it's **Same**-List to the output and set the traversal to the other side. Here we set **LoR** to `DONE` to indicate that one side is already done and we just update **curID** to match the other child. In the other case we update **curID** to indicate we continue with the subtree. *Note:* this represents a recursive call.

The last case is `DONE`. The first one corresponds to a node that has finished both subtrees and therefore the status is set to `DONE`. The latter one indicates a finished subtree and therefore we backtrack to its parent node. *Note:* this would be the return of a recursive call.

The end of the loop writes back the changes to the node and checks if we have arrived at the cell's root node.

5.2.3 Conceptual Error

After having everything set up we re-evaluated the concept of this idea. The property of the BVH-tree — as we constructed it — is also the doom to our idea of usage. Since the triangles are sorted by the Morton codes of their centers' a triangle could potentially spread through multiple cells. Even in that case it would still only end up in one BVH-node. This will essentially lead to errors when sorting since it is not possible to decide if a cell is in front or at the back of another.

Figure 5.12 showcases this problem. On the left we see a scene, which simply contains two overlapping triangles. The yellow and green line mark the bounding boxes of their respective triangles. On the left hand-side of in the scene with have the larger triangle whose result is symbolized as node **A** in the BVH-tree. On the right side we have the triangle in the back and schematically shown as the node **B**. In this case we already struggle to tell if node **A** is in front of node **B** without checking the triangles.

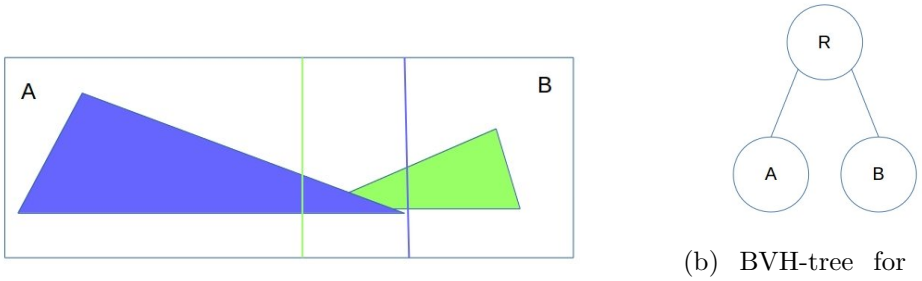

(a) Scene with overlapping triangles

(b) BVH-tree for the scene

Figure 5.12: These images show a scene with overlapping triangles and a possible BVH-tree for the scene

If the nodes contain multiple triangles it is even possible that node **A** contains triangles in front of some in **B** as well as behind those. We therefore would have to merge the sorted list of every node and check those for the order. This results in a big overhead that outweighs the advantages of constructing the small BSP-Trees inside the BVH-nodes.

This realization lead us to think about splitting the scene into smaller cells that can be sorted. A simple solution for this is to lay a grid over the whole scene and split the triangles on the edges.

5.2.4 Grid

We split a scene into small subscenes by lying a uniform grid over it. The size of a cell is the total size of the scene's bounding box divided by the desired number of resulting cells. This procedure is showcased in Figure 5.13. On the left we see an example scene which is to be split. The result of this split is seen in on the right side of the graphic, displaying the cells as circles with their respective BSP-Trees.

During the splitting procedure we come across multiple possible scenarios. The simplest cases are represented by the cells **A** and **E** which consist of only a few triangles. These cells need no further processing. Another simple case is the cell **F** — it is empty and therefore only needs to be removed. Triangles like the one going from cell **B** to **D** and the one in cell **D** and **H** are split into multiple triangles. In the two dimensional case this is similar to the split procedure that we have already used during BSP construction (see Section 5.2.1). In 3D this split is more complicated, yet can be reduced to multiple 2D splits (explanation follows in Section 5.2.4). The last case is a cell like **G**. In general it belongs to the same group as cells **A** and **E**, yet the amount of triangles could lead to problems that will be discussed in Section 5.3.

Sorting

By reducing the scene into non-overlapping cells and doing necessary triangle splitting it is possible to sort the cells. Thus we can sort the cells according to a query and then

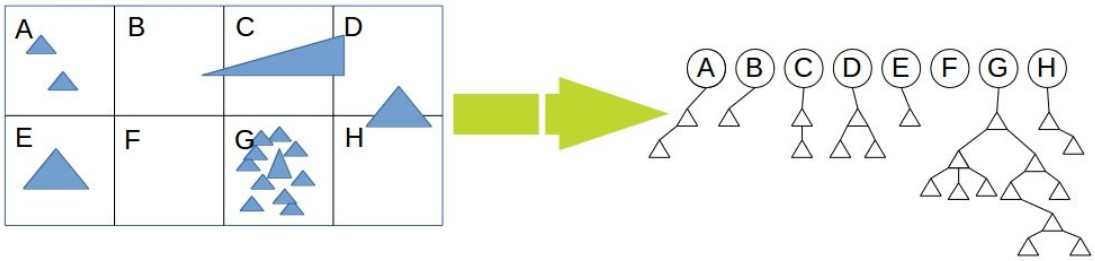

Figure 5.13: The scene on the left on the image is subdivided by a grid into eight cells. The result of this is represented with cells as circles on the right. Each cell contains a BSP-Tree with its triangles. In the compacting step, cell **F** will be removed from the set of cells.

sort the triangles within a cell.

This allows us to make use of the small BSP-Trees. In order to do so we simply process a sorting query by first simultaneously sorting the cells and then forwarding the query to all the BSP-Trees. When the trees complete the procedure we simply have to put their sort results into the order of the cells. Figure 5.14 shows a possible example for our sorting method. In the first image we see the scene and the issued sorting query. Thus we first sort the cells accordingly as show in Figure 5.14b[9]. After that step is completed, we replicate the sorting query to all the cells' BSP-Trees. After traversing them, the last step is adding the triangles to an array in the resulting order.

Polygon splitting

The three-dimensional case of splitting a triangle on a box's planes can lead to several cases. Examples for these cases are shown in Figure 5.15. The simplest case is a triangle contained by a box — here nothing needs to be done (Figure 5.15a). Triangles with all points outside of the box can either contain the box (Figure 5.15d), go through it (Figure 5.15c) or lie on the outside (Figure 5.15b). The first case results in a quad the size of the box. The second scenario yields a quad with the 4 cutting points on the planes. The latter case can be ignored since the triangle does not belong to the cell. Further it is possible that a triangle has points both within and without the box. In this case the split can end up with a polygon having between 3 and 6 edges (Figure 5.15e – Figure 5.15h).

To treat all these possibilities we iterate over the six planes defining the box. For each plane we follow the relevant points of our structure and split its edges on intersections. We add the intersection points to the list of relevant points and continue with the next plane. Via a flag we keep track whether we are currently inside the box or not. This way we cut the polygon on each of the box's faces and obtain a set of points in the end.

[9]Cell **F** was removed from the set of cells because it does not contain any triangles

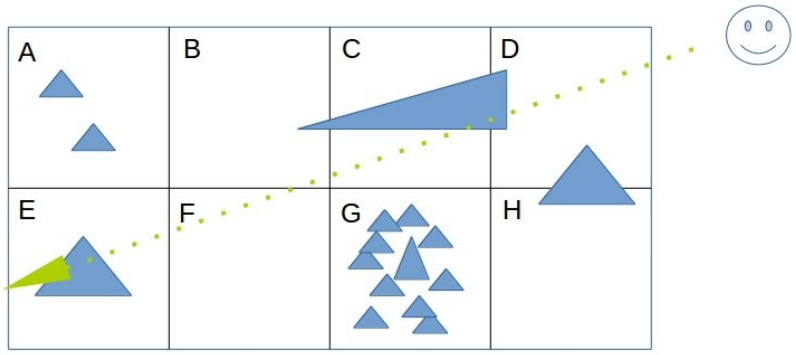

(a) A sorting query is issued to the BSP-grid

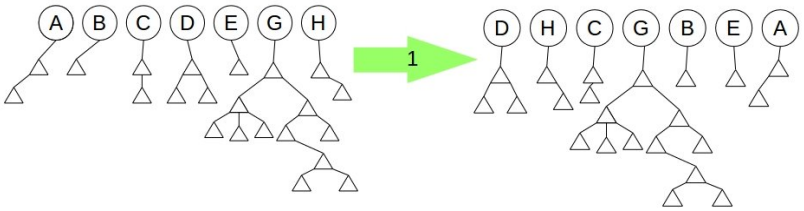

(b) Sorting the cells for the given query

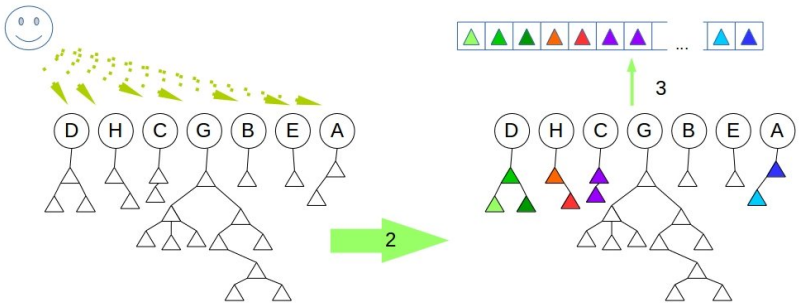

(c) Replicating the query to all BSP-Trees and sorting them

Figure 5.14: Sorting with the BSP-grid

These points form a polygon within the box. To obtain triangles from the polygon a simple traversal, similar to the one shown in Section 5.2.1 is done.

5.3 Limitation Of The GPU

During the implementation we came across certain roadblocks that are specific to the architecture of the GPU. In this section we will showcase the mentioned hindrances and how we solved the resulting problems.

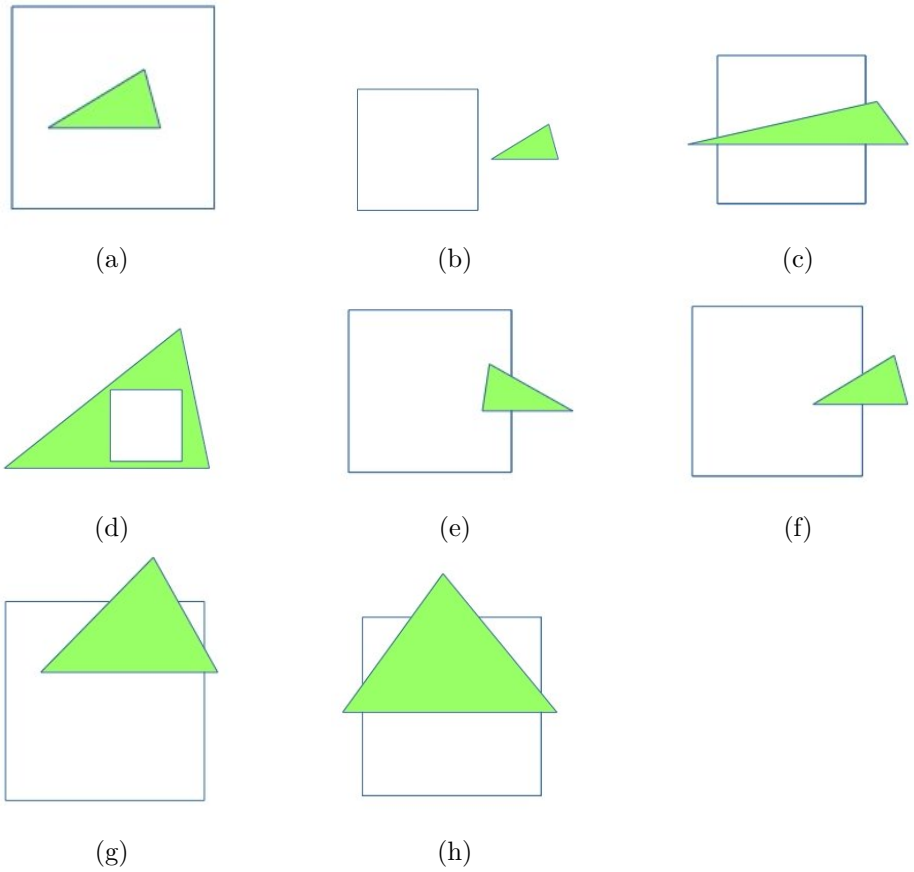

Figure 5.15: Some triangle box intersection possibilities

5.3.1 No Dynamic Memory Allocation

With the OpenCL API it is not possible to dynamically allocate memory within a kernel. That means that the host program needs to know how much memory a kernel needs before executing it. Thus it is not possible to easily use dynamic data-structures such as Lists, Stacks or Queues. This leads to problems whenever we need to generate data. In our case this occurs every time we split a triangle.

As triangle splitting is used both in grid generation as well as during the BSP-Tree build we have to somehow manage the memory accordingly. In the first case we could simply go through the scene and count the amounts of triangles we will have after splitting at cell borders, then allocate according memory before doing the splitting. Although this would deal with the memory allocation problem, we have to run the same code twice because there is no way to know the final number of triangles without going through the split procedure. Thus we opted to preallocate extra memory for every cell and compacted the result in the end. Since we needed to compact anyway to deal with empty cells, we did not create any additional overhead.

In the case of BSP-Tree generation the problem is a more difficult one. Without building the tree, there is no way of knowing how many triangles it will hold in the end. Since we are constructing multiple BSP-Trees at the same time, we also need to consider how we represent the triangles in memory. For this we used the common way, having an array filled with their respective points. Since our algorithm is designed to simply loop over a consecutive set of triangles, we need to add newly generated ones at the end of this set. This means that, for every cell we need to have extra space at the end of the memory range it operates on, so that it can add triangles. We obtained this by spreading out the triangles over the memory and adding a buffer space at the end of every set. Figure 5.16 shows a schematic example of this procedure. The set of blue triangles are put in the first place with extra space next to them. After the end of said buffer space the next set of triangles is placed.

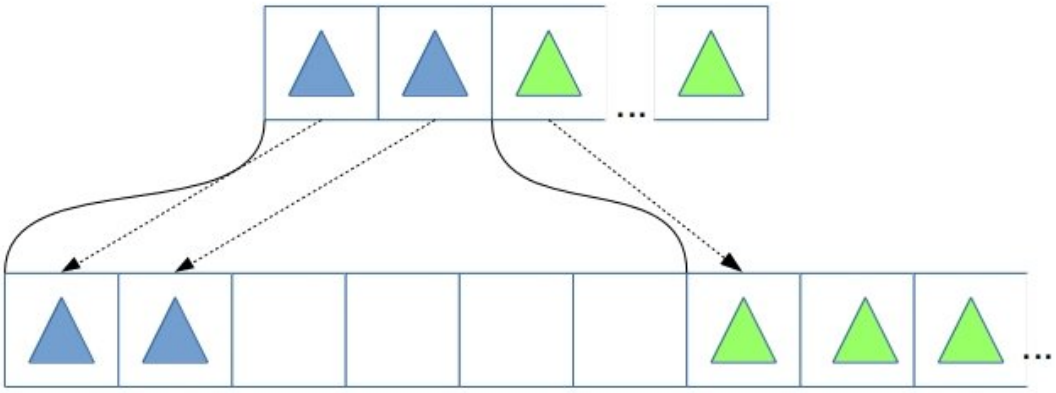

Figure 5.16: Splice out operation on a given set of triangles

Unfortunately for the BSP-Tree there is no simple way to predetermine the additional memory needed and we therefore have to estimate. During testing, 4 times extra buffer space showed to be enough in most cases[10].

5.3.2 Slow Discontinuous Reads And Writes

The memory layout we explained in the previous section leads us directly to the next problem. GPU architectures are very slow when it comes to reading and writing to or from memory locations that are not in order. This manifests itself during our sorting procedure. Since the BSP-grid generation organizes the memory in cell order we have to exactly deal with those discontinuous reads during sorting. During the last step of the sort we have to read the triangle indices in a different order than they are stored. The sparse memory layout further enhances this overhead.

[10] As already mentioned this value is dependent on the number of triangles generated during the build of the BSP-Tree. The latter one — again — is dependent on the size of the grid. Further, the available memory depends on the GPU used. Therefore there is no guarantee that any given number will fit.

We have tried to reorder the final indices in a way to only need to read in consecutive order. Although this should lead to a theoretical speedup, we could not achieve one. This could be due to either the sparse memory layout or the resulting discontinuous writes.

To overcome this problem we added a compacting at the end of the BSP-Tree build. Figure 5.17 shows this procedure, generating an array that does not have any empty cells. Therefore the overall build time increased in favor of the sort time.

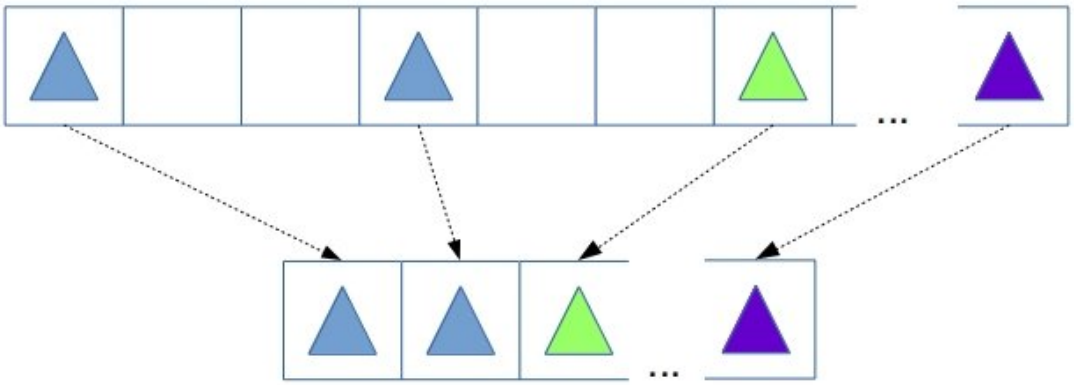

Figure 5.17: Compact operation for a sparse array of triangles

5.3.3 General Memory Limitations

Besides not being able to dynamically allocate memory, we have already hinted toward some other problems in Section 5.3.1. The memory for an OpenCL kernel is very limited. Therefore the sizes of the buffers that are passed to it need to fit those limitations.

In our case this can lead to problems when adapting the size of the grid as it changes the number of triangles per cell. For our implementation it is important to find a good grid size for a given scene. A higher number could lead to too many triangle splits during grid generation that potentially could make us run out of space during said procedure. A smaller number will lead to more triangles per cell and therefore increases the BSP-Tree build time. Further it also leads to more splits during the creation of the tree. This comes with the risk to run out of memory on that end.

During tests we established that a grid size of $n * n * n$ with n between 25 and 35 seems to work well.

CHAPTER 6

Evaluation

We have to evaluate certain properties of the BSP-grid, to see if we can replace the currently used, highly optimized CPU implementation of the BSP-Tree in the Aardvark rendering framework. Most interesting is the sorting performance since transparency sorting the tree's primary use case. Secondly we have to make sure that build times of the BSP-grid are reasonable fast to avoid off-line generation.

Another interesting property is the total amount of triangles we obtain throughout the buildup phase, because we want to keep them as small as possible.

Further we are interested in finding the optimal settings for the BSP-grid. Thus we have examined grid sizes from 1[1] up to 50.

Finally we also searched for weaknesses in our design as well as hardware dependent bottlenecks of our implementation for future improvements.

6.1 Setup

First we give a brief overview of our test setup.

All of our performance tests[2] were run with 10 builds of the chosen implementation with a total of 100 sort operations. Stable results made further iterations unnecessary.

Furthermore we have only used one hardware setup as the prototype was build to test whether this approach can outperform the currently used BSP-Tree or not.

6.1.1 Hardware

For evaluation we used the following hardware

[1] Full single-threaded tree generation on the GPU

[2] Note that the analysis of node selection methods is not a performance test

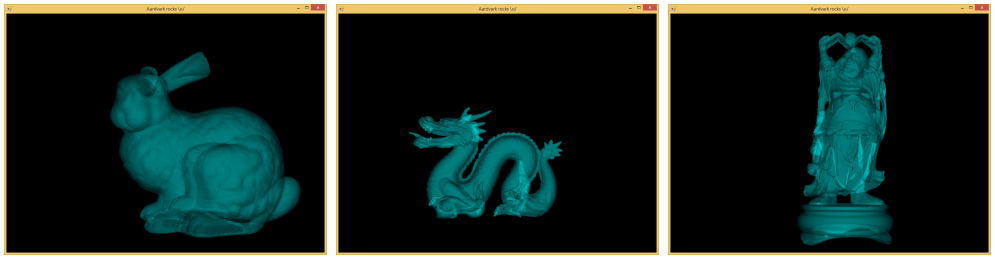

(a) Stanford Bunny (69,451 triangles)

(b) Dragon (1,132,830 triangles)

(c) Happy Buddha (1,087,716 triangles)

Figure 6.1: Models for our evaluation, taken from The Stanford 3D Scanning Repository [sta16]

- **Processor**: Intel Core i5-4690K 3.50 GHz
- **Memory**: 16 GB DDR3 RAM
- **GPU**: GeForce GTX 680, 2048 MB Memory
- **OpenCL**: Version 1.2

6.1.2 Scenes

For our evaluation we took three scenes from **The Stanford 3D Scanning Repository** [sta16] shown in Figure 6.1. The images from the repository are the results of 3D-scans.

These models, being made of many triangles within small region, were selected as they represent our most desired use case, rendering transparency of single objects within a larger scene.

For simplicity we omitted colors and normals from the images, as adding those to the BSP-grid build just add two additional indices to store for each triangle.

6.1.3 Implementations

For the evaluation we used five different implementations as shown in the list below.

GPUGrid This is the implementation as described in the Chapter 5.

CPUGrid-NP A simple CPU implementation of the BSP-grid, without parallelization.

CPUGrid-P As above, but with parallel sorting in the BSP-Trees.

CPU-SingleTree-NP A single BSP tree for the whole scene, omitting the grid.

CPU-SingleTree-P Single tree with parallelization for sorting.

The BSP-grid implementations have a single parameter specifying the grid size. A grid size of n leads to splitting the scene into n^3 cells, before removing the empty ones.

Both CPU implementations of the BSP-grid use the CPU-SingleTree in their grid cells. This tree does not implement a heuristic for building, but simply adds the triangles in input order. The tree construction is quadratically and sorting is linearly proportional to the number of triangles.

The grid generation time in both the GPU and the CPU implementations is proportional to the number of triangles, since we just take each and find cell for it. Building the BSP-Tree in the cells differs between the CPU and the GPU implementation. The CPU implementation uses the CPU-SingleTree and therefore obtains its runtime properties. The GPU implementation, however, originally[3] looped over all triangles quadratically during the build in order to find an appropriate root node for every level[4]. The sort is a simple tree traversal with a theoretical complexity of $O(n)$.

Since we are using parallel algorithms we have to further look how the parallelization plays a role for runtime properties. When parallelized over triangles, the grid generation is dominated by sorting the triangles in cell order, leading to a theoretical complexity of $O(\log n)$[5] for n triangles.

The BSP-Tree generation is parallelized over the grid cells with each of them working on all of their triangles in cubic fashion. The reason for this is that we try to reduce splits by finding the triangle with least splits for every node added in a quadratic loop. For sorting the BSP-Trees we also parallelize over the cells, whereas every cell has to traverse its tree. Hence the runtime is linearly proportional to the number of triangles in every cell. Note that for the BSP-grid the number of triangles per tree is tremendously smaller than for a single BSP-Tree.

6.2 Root Node Selection

During the evaluation we tracked down a bottleneck in the quadratic loop that selects a proper root node at every level of the BSP-Trees. This method was chosen in order to keep the amount of resulting number of triangles as small as possible to be able to stay within the memory limitations of the GPU. As the high build times seemed unreasonable we have inspected the differences in triangle generation between the least splitting method [6] and a simple random select[7]. We evaluated the difference in triangles added for our three test scenes with grid sizes of 25, 30 and 35.

To our surprise, the random select only shows an average increase of 0.15% overall added triangles with respect to the least splitting variant. This value is highly skewed towards

[3] See Section 6.2 why we changed it
[4] See Section 5.2.1 for the implementation
[5] The interested reader is forwarded to Cole's parallel merge sort [Col93]
[6] Explained in Section 5.2.1 as ***findBestSplit***
[7] In fact we are always selecting the triangle which is added last

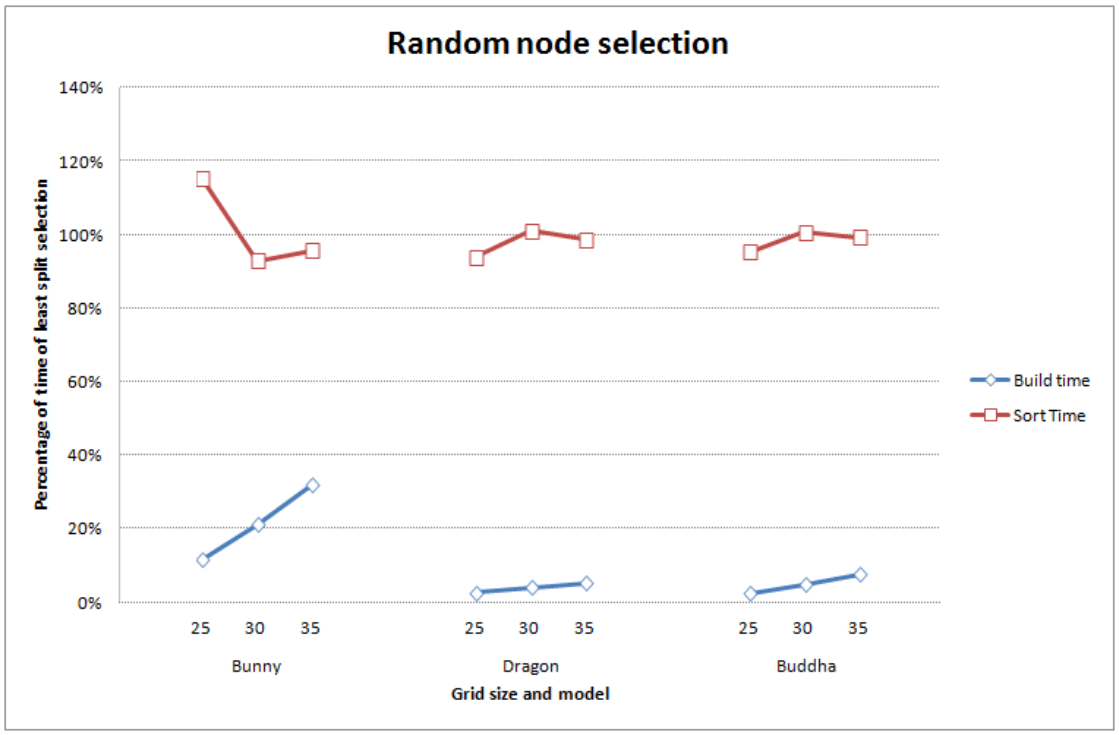

Figure 6.2: The graph shows the relative build and sort times of the random node selection compared to the least-split heuristic. While the sort time almost stayed the same, the build times were strongly reduced by the change.

the Stanford Bunny model which averages at an 0.38% increase. In both the Dragon and the Happy Buddha scenes, the random node selection keeps the increase of triangles below 0.1% for grid sizes of 25 to 35. Figure 6.2 displays the tremendous decrease in build times that we have achieved by ditching the least split selection in favor of the random add method. Further it shows that this does not affect the sort times negatively. The only noticeable increase, was measured for the Stanford Bunny scene with a low grid size. This directly translates from the earlier mentioned increase in generated triangles.

Hence, we changed the implementation to use the random add method for the rest of the evaluation.

6.3 Grid Size

The following tests confirmed our initial hypothesis that with the grid we can achieve faster builds as shown in Figure 6.3a. Interestingly this speedup peaks at a grid size of 25[8]. Thereafter it rises and levels off from 30 onward. We further see that for the larger

[8] As we will see later in this section, the number of triangles per cell stay steady for higher grid sizes.

two test scenes the build time drastically falls off for grid sizes smaller than 20 as the triangles per cell fall off the most here.

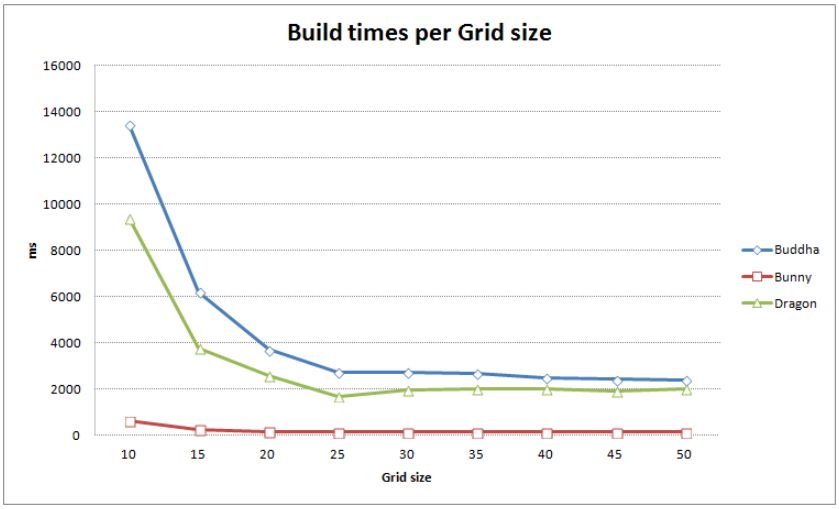

(a) Build times

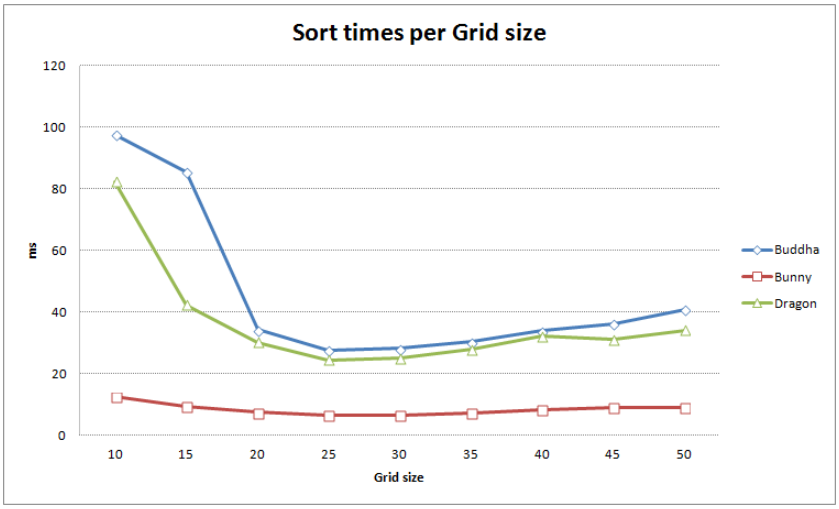

(b) Sort times

Figure 6.3: These graphs show the build (a) and the sort times (b) in milliseconds for different grid sizes. Here we see, that in our setup the grid size of 25 performs best over all the scenes

Interestingly the sorting times behaved the same, as shown in Figure 6.3b. Our test results showed that after a certain peak — typically around grid sizes of 25 — the sorting times increase again. Figure 6.4 displays that a possible reason for this could be that separating the scene into *too many* cells leads to a huge amount of triangle splits. As

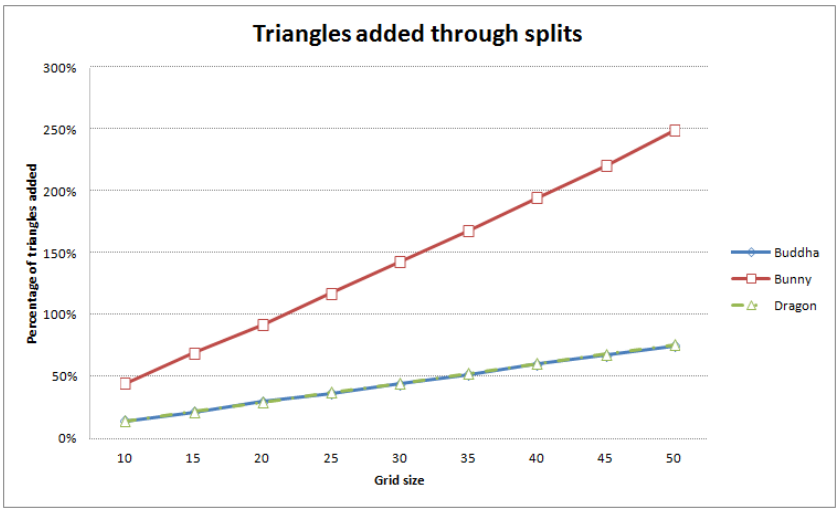

Figure 6.4: Here we can see the relative amount of triangles generated through splits for different grid sizes. The displayed linear growth suggests that increasing number of cells translate into more triangle splits and thus not reducing the overall problem size anymore.

we can see in the graph the amount of newly-added triangles is linearly related to the number of cells. This linear trend leads to problems when we surpass a certain threshold. The Stanford Bunny test scene reached the value of 250% newly-generated triangles with a grid size of 50. From that point on we have to omit triangles as we run out of buffer space in our test setup.

We have also found out that the BSP-Trees generated less than 1% of the overall new triangles during our tests.

Thus from a certain cell count onward the number of triangles per BSP-Tree does not decrease anymore, because smaller cells lead to more triangle splits during grid generation. Since increasing the number of cells with a decreasing number of triangles per cell will also inevitably lead to having the number of cells overtake the number of triangles, we inspected the relation between the number of triangles and cells.

Figure 6.5 shows that averaged over our test scenes the number of cells overtake the number of containing triangles already with a grid size of 15. We further noticed that at our favored grid size of 25 we reach a triangle count lower than 300 per cell and stayed around the same value thereafter.

6.4 Comparing Implementations

Our second test benchmarked the different implementations against each other. For this we only took grid sizes between 25 and 35 as these seem to achieve the best results. We further used the CPUGrid-NP as our baseline to test against.

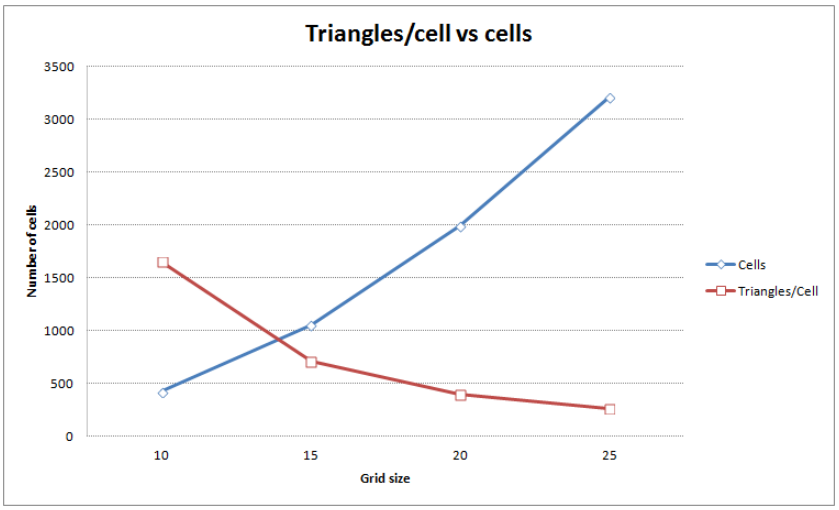

Figure 6.5: This graph shows the relation between the number of cells and the average triangles per cell. We can see that the number of cells surpasses the number of triangles within them at low grid sizes already. Further from 25 the number of triangles per cell reaches a lower limit.

As we can see in the first graph in Figure 6.6 the build times are dominated by our GPUGrid. Interestingly the GPU implementation of the BSP-grid achieves the highest speedup in the smallest scene. It is also interesting to see that a single BSP-Tree outperforms the CPU implementation of the BSP-grid. The reason for this is that the CPU-SingleTree does not need to reorder data and combine it, as this is costly if not done in parallel.

Table 6.1 shows the sort times compared to the CPUGrid-NP baseline[9]. To our surprise the CPUGrid seems to perform worse when the BSP-Trees sort in parallel. A possible explanation for this is, that organizing parallel execution for small instances outweighs the actual sorting costs. The sort times for the CPU-SingleTree, that always works on the whole scene, confirm this assumption by showing that the parallel version outperforms its non-parallel counterpart.

Figure 6.6b shows the performance gain of our GPU implementation and the CPU-SingleTree-NP compared to the CPUGrid-NP baseline. We can see, that the GPU BSP-grid sorts faster for all our test cases. Interestingly the performance gain for the Happy Buddha scene increases with the grid size. This abnormality seems to be scene specific as the number of triangles per cell as well as both their total numbers do not suggest any correlation[10].

Unfortunately we could not manage to outperform the highly optimized BSP-Tree when used as standalone variant.

[9] Note that CPU-SingleTree, by construction, is not influenced by the grid size

[10] Possibly the triangles are not evenly distributed throughout the cells

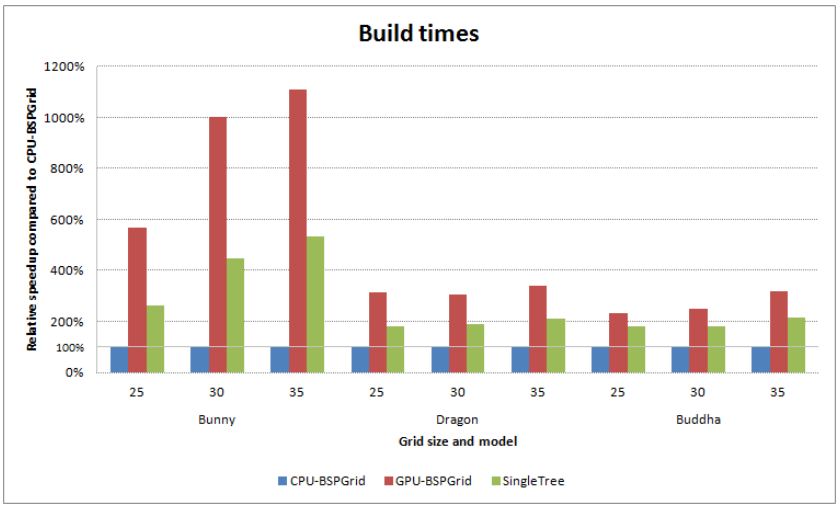

(a) Build times

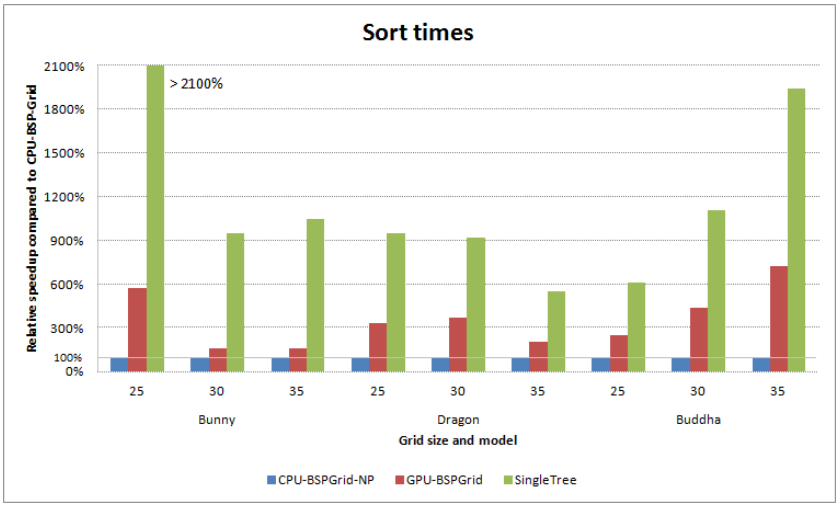

(b) Sort times

Figure 6.6: These graphs show the relative speedup of build (a) and sort times (b) compared to a baseline CPU implementation. Here we can see that our GPU implementation of the BSP-grid not only outperforms the CPU baseline, but also builds consistently faster than the CPU-SingleTree variant.

6.4.1 Limitations

A core limitation of our setup is the memory the GPU has to offer. This means that — as already mentioned in Section 6.3 — certain instance sizes and configurations lead to the problem of running out of buffer space. During our test this happened when we created more than 250% of the original scene triangles. In those cases we have to omit triangles,

GS	CPUGrid-NP	CPUGrid		GPUGrid		CPU-SingleTree-NP		CPU-SingleTree-P	
					Bunny				
25	37,54	44,57	84%	6,57	571%	1,11	3389%	0,47	8036%
30	10,54	24,37	43%	6,49	162%	1,11	952%	0,47	2257%
35	11,61	34,32	34%	7,37	158%	1,11	1049%	0,47	2486%
					Dragon				
25	97,14	70,40	138%	29,12	334%	10,22	951%	5,76	1688%
30	93,99	77,21	122%	25,34	371%	10,22	920%	5,76	1633%
35	56,23	108,53	52%	27,62	204%	10,22	550%	5,76	977%
					Buddha				
25	68,90	78,13	88%	27,61	250%	11,21	615%	5,84	1179%
30	124,19	86,824	143%	28,50	436%	11,218	1108%	5,84	2125%
35	217,68	245,68	89%	30,18	721%	11,21	1943%	5,84	3725%

Table 6.1: Sorting times in ms and relative performance gain compared to the baseline CPUGrid-NP

making the result incorrect. This also can happen for very unbalanced scenes with many triangles in a single cell as those will likely split more and therefore overrun the buffer space.

Another problem is that scenes with more than 2.5 million triangles will not work with the current setup. This could be fixed by further analyzing memory footprints and adapting buffer sizes during the build of the BSP-grid.

6.4.2 Conclusion

Throughout these benchmarks we have learned that the GPU implementation performs best with a grid size around 25.

After a grid size of 35 we could not see any drastic improvements in sorting for our hybrid approach. However by applying the random split node selection strategy we can outperform the CPU implementation as well as the CPU-SingleTree during build times for grid sizes of 15 and above.

Unfortunately we could not outperform the CPU-SingleTree-NP as originally fancied. Nonetheless, for sorting, our hybrid approach could almost perform on par with it. Further our GPUGrid offers the additional advantage, that it omits the data transfer between CPU and GPU.

CHAPTER 7

Conclusion and Future Work

We presented a hybrid approach for BSP-Tree generation on the GPU. Our algorithm combines a simple uniform grid and a common BSP-Tree. The so-called BSP-grid is then fully sortable and achieves reasonable sort times.

By splitting the scene into multiple subscenes we decreased the instance sizes for BSP-Tree construction tremendously. With this reduction it is possible to build a BSP-grid in feasible time for a given scene.

Throughout the implementation process of our algorithm we came across different roadblocks. Originally we planned on making use of the well-researched BVH-trees for frustum culling. As established during implementation we could not use them to lower the complexity for said problem.

We then tried to obtain a scene splitting by making use of a BVH-tree in Karras' [Kar12] fashion. Since this tree is designed to *roughly* sort the primitives of a scene, it is not possible to use it for transparency sorting. Further the limitations of GPU programming take their toll during the BSP-grid building phase.

For our implementation we used an F# to OpenCL cross-compiler[1] for simpler embedding into the current framework. This way the code is not only cleaner, but also more easily maintainable.

Evaluation showed that we could outperform a CPU implementation by a large margin. We further found out that an increasing grid sizes benefit the BSP-grid only up to a certain point. Thus we pinpointed this value at 25 for the current settings.

Our approach further offers the advantage that it is fully implemented on the GPU, meaning there is no need for data transfer between GPU and CPU.

[1] See Section 4.5

7.1 Future Work

Our implementation offers huge optimization potential. First of all it might be possible to reduce memory usage by precalculating and estimating triangle splits for grid and BSP-Tree generation respectively. Further the memory layout could be changed to reduce splicing and compacting operations.

Another weak point of the algorithm is the BSP-Tree generation itself. Its complexity was already reduced by omitting the root node selection. However, this might lead to situations where we run out of buffer memory. With a different memory layout it might also be possible to add the triangles in different ways than simply looping through them.

Further we believe that with certain adaptions the BVH-tree can be used instead of the grid. This could possibly be done by altering its construction process to employ triangle splitting.

Lastly it might be possible to create smaller subscenes by using an octree instead of a grid. This way the scene could be recursively split until cells reach a certain limit of triangles to process, thus creating the possibility to further optimize the BSP-Trees themselves.

List of Figures

1.1 Ray tracing example 2
1.2 Transparency sorting example 2

3.1 Painter's algorithm Problem 9
3.2 Transparency sorting example 10
3.3 Ray tracing schematic example 11
3.4 Ray traced image example 12
3.5 Transparency sorting example 12
3.6 Karass' radix tree design 15
3.7 BSP example 19
3.8 k-d tree construction pattern 20
3.9 Tree summation illustration 22

4.1 OpenCL architectural model 26
4.2 OpenCL 2-dimensional work structure grid 27
4.3 OpenCL Memory hierarchy 27
4.4 OpenCL Memory synchronization 28
4.5 OpenCL event queue 28
4.6 OpenCL Matrix multiplication 29
4.7 F# Matrix multiplication 30
4.8 F# host program 31

5.1 Top level BVH builder 35
5.2 Kernel of the core function for BVH construction 36
5.3 Function to determine the range of an internal node 37
5.4 Triangle split result 40
5.5 Definition of BSPNode 41
5.6 Kernel for building the BSP-Tree 42
5.7 Evaluation loop of the kernel 43
5.8 Next level preparation section of the kernel 44
5.9 Triangle splitting example 46
5.10 Kernel ***sortBSPTreeKernel*** 47
5.11 Internal node part of ***sortBSPTreeKernel*** 48
5.12 Conceptual Errors 50

5.13 Grid Generation example 51
5.14 BSP-grid sorting example 52
5.15 Triangle Box intersections 53
5.16 Array splice out 54
5.17 Array compact 55

6.1 Test scenes 58
6.2 Node selection build and sort times 60
6.3 Build and sort times for different grid sizes 61
6.4 Triangles generated for different grid sizes 62
6.5 Triangles per cell chart 63
6.6 Build and sort times for different implementations 64

List of Tables

6.1 Sort time comparison 65

List of Algorithms

3.1 SIMD tree summation 21

4.1 Matrix multiplication 28

Bibliography

[Ado] Adok. 2d ray tracing example.

[AKL13] Timo Aila, Tero Karras, and Samuli Laine. On quality metrics of bounding volume hierarchies. In *High-Performance Graphics 2013, Anaheim, California, USA, July 19-21, 2013. Proceedings*, pages 101–108, 2013.

[AMD] AMD. Ati mecha demo screenshot.

[App68] Arthur Appel. Some techniques for shading machine renderings of solids. In *American Federation of Information Processing Societies: AFIPS Conference Proceedings: 1968 Spring Joint Computer Conference, Atlantic City, NJ, USA, 30 April - 2 May 1968*, pages 37–45, 1968.

[Ary02] Sunil Arya. Binary space partitions for axis-parallel line segments: Size-height tradeoffs. *Inf. Process. Lett.*, 84(4):201–206, 2002.

[AT10] Nathan Andrysco and Xavier Tricoche. Matrix trees. *Comput. Graph. Forum*, 29(3):963–972, 2010.

[AT11] Nathan Andrysco and Xavier Tricoche. Implicit and dynamic trees for high performance rendering. In *Proceedings of the Graphics Interface 2011 Conference, May 25-27, 2011, St. John's, Newfoundland, Canada*, pages 143–150, 2011.

[BCNJ08] B. C. Budge, D. Coming, D. Norpchen, and K. I. Joy. Accelerated building and ray tracing of restricted bsp trees. In *Interactive Ray Tracing, 2008. RT 2008. IEEE Symposium on*, pages 167–174, Aug 2008.

[BHH15a] Jirí Bittner, Michal Hapala, and Vlastimil Havran. Incremental BVH construction for ray tracing. *Computers & Graphics*, 47:135–144, 2015.

[BHH15b] Jirí Bittner, Michal Hapala, and Vlastimil Havran. Incremental BVH construction for ray tracing. *Computers & Graphics*, 47:135–144, 2015.

[CF89] Norman Chin and Steven Feiner. Near real-time shadow generation using BSP trees. In *Proceedings of the 16th Annual Conference on Computer Graphics and Interactive Techniques, SIGGRAPH 1989, Boston, MA, USA, July 31 - August 4, 1989*, pages 99–106, 1989.

[CKL+10] Byn Choi, Rakesh Komuravelli, Victor Lu, Hyojin Sung, Robert L. Bocchino Jr., Sarita V. Adve, and John C. Hart. Parallel SAH k-d tree construction. In *Proceedings of the ACM SIGGRAPH/EUROGRAPHICS Conference on High Performance Graphics 2010, Saarbrücken, Germany, June 25-27, 2010*, pages 77–86, 2010.

[Col93] Richard Cole. Correction: Parallel merge sort. *SIAM J. Comput.*, 22(6):1349, 1993.

[EG07] M. Ernst and G. Greiner. Early split clipping for bounding volume hierarchies. In *2007 IEEE Symposium on Interactive Ray Tracing*, pages 73–78, Sept 2007.

[FKN80] Henry Fuchs, Zvi M. Kedem, and Bruce F. Naylor. On visible surface generation by a priori tree structures. In *Proceedings of the 7th Annual Conference on Computer Graphics and Interactive Techniques, SIGGRAPH 1980, Seattle, Washington, USA, July 14-18, 1980*, pages 124–133, 1980.

[FS05] Tim Foley and Jeremy Sugerman. Kd-tree acceleration structures for a GPU raytracer. In *Proceedings of the ACM SIGGRAPH/EUROGRAPHICS Symposium on Graphics Hardware 2005, Los Angeles, California, USA, July 30-31, 2005*, pages 15–22, 2005.

[GHFB13] Yan Gu, Yong He, Kayvon Fatahalian, and Guy E. Blelloch. Efficient BVH construction via approximate agglomerative clustering. In *High-Performance Graphics 2013, Anaheim, California, USA, July 19-21, 2013. Proceedings*, pages 81–88, 2013.

[gpg] General-purpose computing on graphics processing units.

[GS87] Jeffrey Goldsmith and John Salmon. Automatic creation of object hierarchies for ray tracing. *IEEE Computer Graphics and Applications*, 7(5):14–20, 1987.

[Hav00] Vlastimil Havran. *Heuristic ray shooting algorithms.* PhD thesis, Citeseer, 2000.

[HBZ98] Vlastimil Havran, Jirí Bittner, and Jirí Zára. Ray tracing with rope trees. In *in Proceedings of 13th Spring Conference On Computer Graphics, Budmerice in Slovakia*, pages 130–139, 1998.

[Hen08] Henrik. Ray traceing diagram, 2008.

[HL09] David M. Hughes and Ik Soo Lim. Kd-jump: a path-preserving stackless traversal for faster isosurface raytracing on gpus. *IEEE Trans. Vis. Comput. Graph.*, 15(6):1555–1562, 2009.

[HS03] John Hershberger and Subhash Suri. Binary space partitions for 3d subdivisions. In *Proceedings of the Fourteenth Annual ACM-SIAM Symposium on Discrete Algorithms, January 12-14, 2003, Baltimore, Maryland, USA.*, pages 100–108, 2003.

[imga] 3d ray tracing example.

[imgb] Binay space partitioning example.

[IWP07] Thiago Ize, Ingo Wald, and Steven G. Parker. Asynchronous BVH construction for ray tracing dynamic scenes on parallel multi-core architectures. In *Eurographics Symposium on Parallel Graphics and Visualization, EGPGV 2007, Lugano, Switzerland, May 20-21, 2007*, pages 101–108, 2007.

[IWP08] T. Ize, I. Wald, and S. G. Parker. Ray tracing with the bsp tree. In *Interactive Ray Tracing, 2008. RT 2008. IEEE Symposium on*, pages 159–166, Aug 2008.

[KA13] Tero Karras and Timo Aila. Fast parallel construction of high-quality bounding volume hierarchies. In *High-Performance Graphics 2013, Anaheim, California, USA, July 19-21, 2013. Proceedings*, pages 89–100, 2013.

[Kar12] Tero Karras. Maximizing parallelism in the construction of bvhs, octrees, and k-d trees. In *Proceedings of the EUROGRAPHICS Conference on High Performance Graphics 2012, Paris, France, June 25-27, 2012*, pages 33–37, 2012.

[KIS+12] Daniel Kopta, Thiago Ize, Josef B. Spjut, Erik Brunvand, Al Davis, and Andrew E. Kensler. Fast, effective BVH updates for animated scenes. In *Symposium on Interactive 3D Graphics and Games, I3D '12, Costa Mesa, CA, USA, March 09 - 11, 2012*, pages 197–204, 2012.

[LGS+09] Christian Lauterbach, Michael Garland, Shubhabrata Sengupta, David P. Luebke, and Dinesh Manocha. Fast BVH construction on gpus. *Comput. Graph. Forum*, 28(2):375–384, 2009.

[MB90] J. David MacDonald and Kellogg S. Booth. Heuristics for ray tracing using space subdivision. *The Visual Computer*, 6(3):153–166, 1990.

[Muł] Wojciech Muła. Painters problem.

[PL10] Jacopo Pantaleoni and David Luebke. HLBVH: hierarchical LBVH construction for real-time ray tracing of dynamic geometry. In *Proceedings of the ACM SIGGRAPH/EUROGRAPHICS Conference on High Performance Graphics 2010, Saarbrücken, Germany, June 25-27, 2010*, pages 87–95, 2010.

[SBU11] D. Sopin, D. Bogolepov, and D. Ulyanov. Real-time sah bvh construction for ray tracing dynamic scenes. 2011.

[Sch] Schreiberx. Bounding volume hierarchy example.

[SD69] R. Schumacher and Air Force Human Resources Laboratory. Training Research Division. *Study for Applying Computer-generated Images to Visual Simulation*. AFHRL-TR. Air Force Human Resources Laboratory, Air Force Systems Command, 1969.

[SSK07] Maxim Shevtsov, Alexei Soupikov, and Alexander Kapustin. Highly parallel fast kd-tree construction for interactive ray tracing of dynamic scenes. *Comput. Graph. Forum*, 26(3):395–404, 2007.

[sta16] The stanford 3d scanning repository, 2016.

[Tót05] Csaba D Tóth. Binary space partitions: Recent developments. *Combinatorial and Computational Geometry. MSRI Publications*, 52:529–556, 2005.

[Träa] Jesper Larsson Träff. Summation on the pram example.

[Trab] Gilles Tran. Glasses, persistence of vision raytracer (pov ray) - hall of fame.

[TS12] Jonathan Tompson and Kristofer Schlachter. An introduction to the opencl programming model. *Person Education*, 2012.

[USC13] Murat Uysal, Baha Sen, and Canan Celik. Hidden surface removal using bsp tree with cuda. *Global Journal on Technology*, 3(0), 2013.

[Vog13] Günther Voglsam. Real-time ray tracing on the gpu -ray tracing using cuda and kd-trees, 2013.

[Wal07] Ingo Wald. On fast construction of sah-based bounding volume hierarchies. In *Proceedings of the 2007 IEEE Symposium on Interactive Ray Tracing*, RT '07, pages 33–40, Washington, DC, USA, 2007. IEEE Computer Society.

[WBKP08] B. Walter, K. Bala, M. Kulkarni, and K. Pingali. Fast agglomerative clustering for rendering. In *Interactive Ray Tracing, 2008. RT 2008. IEEE Symposium on*, pages 81–86, Aug 2008.

[Whi79] Turner Whitted. An improved illumination model for shaded display. In *Proceedings of the 6th Annual Conference on Computer Graphics and Interactive Techniques, SIGGRAPH 1979, Chicago, Illinois, USA, August 8-10, 1979*, page 14, 1979.

[Woo04] Sven Woop. *A ray tracing hardware architecture for dynamic scenes*. PhD thesis, Universität des Saarlandes, 2004.

[WZL11a] Zhefeng Wu, Fukai Zhao, and Xinguo Liu. SAH kd-tree construction on GPU. In *Proceedings of the ACM SIGGRAPH/EUROGRAPHICS Conference on High Performance Graphics 2011, Vancouver, Canada, August 5-7, 2011*, pages 71–78, 2011.

[WZL11b] Zhefeng Wu, Fukai Zhao, and Xinguo Liu. SAH kd-tree construction on GPU. In *Proceedings of the ACM SIGGRAPH/EUROGRAPHICS Conference on High Performance Graphics 2011, Vancouver, Canada, August 5-7, 2011*, pages 71–78, 2011.

[YYWX16] Xin Yang, Bing Yang, Pengjie Wang, and Duanqing Xu. MSKD: multi-split kd-tree design on GPU. *Multimedia Tools Appl.*, 75(2):1349–1364, 2016.

[ZHWG08] Kun Zhou, Qiming Hou, Rui Wang, and Baining Guo. Real-time kd-tree construction on graphics hardware. *ACM Trans. Graph.*, 27(5):126, 2008.